Fatigue life prediction of bolt in preloaded connection for FRP composite deck

Through in-situ monitoring and finite element modelling

TU Delft

Bas Berger

Fatigue life prediction of bolt in preloaded connection for FRP composite deck

Through in-situ monitoring and finite element modelling

by

Bas Berger

to obtain the degree Master of Science
in Structural Engineering
at the Delft University of Technology

Student number: 4489888

Thesis committee:

Dr. M. Pavlović,	*Chairman*
Ir. A. Christoforidou,	*Daily supervisor*
Ir. M. Koetsier,	*Daily supervisor*
Dr. Y. Yang,	*External committee member*

PREFACE

This thesis marks the final step in completing my Master of Science degree in Civil Engineering at TU Delft. Firstly I want to express my appreciation for the members of my thesis committee. I would like to thank the chairman of my committee, Marko Pavlovic, for his guidance and support during this period. I would also like to thank my daily supervisors, Angeliki Christoforidou and Mathieu Koetsier, availability, feedback and especially for travelling to the Ulsderbrug in Groningen with me when this was required for the monitoring of the bridge. I also want to thank Yuguang Yang, my external committee member, for being part of my thesis committee.

Secondly I would also want to thank the people that helped me build and maintain the monitoring system used at the bridge. I would like to thank the staff at the TU Delft laboratory for helping me build a remotely accessible monitoring system and helping me with its installation at the bridge. I would also like to express my gratitude to Jan Hiddingh from the Province of Groningen, who was always will to check at the bridge when technical issues occurred.

Finally I would like to thank my family and friends for their encouragement and support throughout this period.

Bas Berger

Lelystad, July 2025

ABSTRACT

A large part of the bridges in the Netherlands have been built in the 50s and 60s of the last century. These bridges have to be renovated because they are reaching the end of their designed lifespan and they are not designed for the more and heavier current traffic This is especially relevant for the steel bridges because this could lead to problems due to fatigue. A common method for renovating the bridge is by using a FRP bridge deck, which has a high strength to weight ratio and have good fatigue resistance. Since this is a relatively new method, a lot of research has been done for connection methods between the FRP bridge deck and the steel superstructure of the bridge. Two example of these connectors are the Lindapter Hollo bolted connector and the iSRR connector, which are both blind-bolted connectors. The iSRR connector uses steel reinforced resin to create an efficient, slip-resistant connection. This a relatively new connection method, therefore there is not a lot of knowledge about the long-term behavior of this connector. To investigate this, the iSRR connector has been installed alongside the Lindapter Hollo bolted connector at the Ulsderbrug in Groningen. These preloaded connectors are designed in such a manner that they only transfer tensile forces. These bolted connectors are monitored to compare both the short-term and long-term behavior. In addition to the monitoring a finite element model is made, to investigate to predictability of the bolt forces in the iSRR connector.

From the monitoring can be concluded that the iSRR connector shows less loss of preload over a period of 250 days, retaining 50.6% of the original preloading force. Compared to 42.7% for the Lindapter Hollo bolted connector. These losses of preload are significantly impacted by a rubber interlayer that is present between the clamping plate and the FRP bridge deck. Due to the relaxation of this rubber layer, only 77.5% of the applied preloading force is present one day after applying. The force variations, of up to 0.12 kN, due to traffic loads are relatively small and similar for both connector types. These forces are also affected by the rubber interlayer. Imperfections at these layers cause one bolt to experience force cycles up to 1.2 kN, which are ten times higher than for the other bolts. The influence of the stiffness of the rubber interlayer has been investigated using the finite element model. From this model can concluded that a lower stiffness of this layer leads to higher forces in the connectors. This model has been used to investigate the extrapolate the bolt forces for the most unfavorable stiffness of the rubber. Even for this conditions the lifespan of the bolts and the connectors is not affected by the forces due to traffic loading.

In conclusion, the results show that the iSRR bolts retains more of the applied preloading force over a long period than the Lindapter Hollo bolts. Short-term behavior has been similar between the bolts but has significantly been impacted by a rubber interlayer between the clamping plate and the FRP bridge deck. For further research it would be interesting to optimize the positioning of the rubber layer and investigate how this impacts the results.

Contents

1. Introduction 1
1.1 Problem statement 2
1.2 Research questions 3
1.3 Methodology 4
2. Literature review 5
2.1 FRP decks 5
2.1.1 Pultruded FRP Decks 5
2.1.2 Sandwich decks 7
2.2 Connection methods for FRP decks 9
2.2.1 Adhesive connectors 9
2.2.2 Bolted connectors 9
2.2.3 Blind bolted connectors 10
2.2.4 iSRR connector 12
3. Bridge monitoring 14
3.1 Bridge characteristics 14
3.1.1 Superstructure of the bridge 14
3.1.2 FRP bridge deck 16
3.1.3 iSRR connector 17
3.1.4 Lindapter Hollo bolt connector 18
3.1.5 Preloading of the bolts 19
3.2 Measurement of bolt forces 20
3.3 Monitoring set up at the bridge 23
3.4 Measurement settings 24
4. Results 25
4.1 Traffic loading 25
4.1.1 Vehicle load 25
4.1.2 Influence of the velocity of the truck 26
4.1.3 Lindapter Hollo bolt connector 28
4.1.4 iSRR connector 29
4.1.4 Comparison of the connectors 30
4.1.5 Hypothesis deviation bolt 2 31
4.2 Opening of the bridge 33

4.2.1 Bolt forces before re-preloading 33
4.2.2 Bolt forces after re-preloading 33
4.2.3 Comparison between the iSRR and Hollo connectors 34
4.3 Influence of the temperature 35
4.4 Loss of preload 36
4.4.1 Lindapter Hollo bolts 37
4.4.2 iSRR bolts 39
4.4.3 Comparison for both types of connectors 40
4.5 Long-term effects 42
5. Finite Element Model 45
5.1 Model definition 45
5.2 Analysis 50
5.3 Limitations of the model 51
5.4 Verification 52
5.5 Sensitivity 57
6. Conclusions 57
7. Recommendations 58
Bibliography 59
Annex A Dimensions of the girder and crossbeam 61

1. Introduction

In the Netherlands, the Ministry of Infrastructure, Rijkswaterstaat, is responsible for several bridges. Because a large part of these bridges was built in the 50s and 60s of the last century, many bridges have to be renovated. This is because they are reaching the end of their designed lifespan, but also because they are increasingly intensively loaded by more and heavier traffic. In particular the increase in intensity and weight of the freight traffic has an important effect on the lifespan of the bridges (Schultz van Haegen-Maas Geesteranus, 2016). Especially in steel bridges this has a large effect because it could lead to problems due to fatigue. Because of this, a peak in the number of bridges that need to be renovated is expected in the next 30 years. Over the next 15 years, Rijkswaterstaat will carry out smaller and large-scale replacements and renovations to approximately 175 movable bridges (Rijkswaterstaat, 2021).

These bridges have different types of bridge decks, the decks can be made of concrete, wood, or orthotropic material. One of the options to improve the strength of the deck is to replace the existing deck is with Fibre Reinforced Polymer (FRP) panels. The advantage of this is that they are lightweight, have good fatigue resistance and do not suffer from stress rupture compared with glass or aramid fibers (Pipinato, Pellegrino, & Modena, 2012). But because this is a relatively new method little is known about the long-term performance of the connectors of the deck and the steel substructure of the bridge. Two types of connectors between the FRP deck and steel substructure are the injected steel reinforced resin connector (iSRR) and the Lindapter bolt connector. Both types of connectors are more elaborately discussed in chapter 2. There is more knowledge about the Lindapter bolt connector since this is a more traditional connection method between a FRP bridge deck and the steel superstructure of the bridge, but because the iSRR connector is relatively new more knowledge is needed about the performance of this connector. To become more familiar with these connectors, both types of connectors between the FRP deck and the steel bridge substructure are attached to the same bridge. This bridge is the Ulsderbrug located in Groningen. Because this bridge has been made available by the province of Groningen, it is possible to monitor these connectors and compare the real-life performance.

1.1 Problem statement

The knowledge about long-term performance of connectors between a FRP deck and the substructure of a steel bridge is still limited. This is the case because the use of a FRP deck is a relatively new method for bridges and steel to steel interventions were privileged up to now (Pipinato, Pellegrino, & Modena, 2012). Therefore research should be done about the short and long-term performance of these connectors.

A FRP deck has a very good fatigue resistance but the fatigue behaviour of FRP is also less predictable than the fatigue behaviour of steel. This is because unlike steel FRP has multiple damage mechanisms (M. Fotouhi, 2015). Therefore it is very useful to monitor the long-term effects for different types of connectors between a FRP deck and the steel substructure of the bridge to gain information about the fatigue life of the bridge.

This study is focussed on tensile forces in the connectors. Two types of bolted connectors will be monitored at the Ulsderbrug. Half of the connectors is connected via the traditional way, the Lindapter Hollo bolt with an internal steel plate. The other connectors used are injected steel reinforced resin connectors (iSRR). This is a new type of connector that is being developed at the TU Delft. The goal of this connector is to utilise the improved properties of SRR injection to provide a slip resistant and fatigue enduring connection by combining the injection and preloading of the bolt (Olivier, Csillag, Tromp, & Pavlovic, 2021). Both connectors are designed using a clamping plate. Due to this clamping plate the connectors are only able to transfer tensile forces.

The aim of this study is to gain knowledge about the performance of an iSRR connector loaded purely in tension as a connector between a FRP deck and the steel substructure of the bridge. With the results of testing and monitoring conclusion can be made about the performance of the iSRR connector and it can be compared to the performance of a more traditional Lindapter blind-bolted connector.

1.2 Research questions

From the problem analysis the main research question for this master thesis, along with additional sub-questions, can be formulated.

Main research question:

What is the difference in short-term and long-term behaviour of the in-situ iSRR connector and the traditional Lindapter bolted connector when both, as a bridge-deck connector, are only loaded in tension?

Sub research questions:

How can the in situ tensile forces at the bridge be monitored?

What are the maximum and minimum forces that occur in both connectors monitored during real loading conditions at the bridge?

For the fatigue performance of the connectors it is important to know the magnitude of the maximum and minimum forces in the connectors and see for which type of connector they are more favourable.

Is there a difference in loss of the preload between the iSRR connector and the Lindapter connector?

Investigating the loss of preload is important because there is a direct relation between the preload of the bolt and the resistance of the connector.

What is the difference between the predicted force changes and the occurring force changes?

It is useful to look at how well occurring load cycles due to a truck passing the bridge can be predicted to know how accurately predictions can be done in the future.

1.3 Methodology

To be able to compare the tensile forces in both connectors and therefore answer the research questions several steps have to be taken. First literature will be studied to become more familiar with the types of connectors used, other connector types and FRP decks. After this, a remote monitoring system will be designed and built in the Stevin 2 lab at the TU Delft. This monitoring system will be set up at the Ulsderbrug in Groningen to measure the short-term and long-term effects. Four Lindapter connectors and four iSRR connectors will be monitored. With the monitoring, the force cycles in the bolts due to traffic, opening and closing of the bridge, and temperature will be measured. After the monitoring system has been installed, a finite element method model will be created of the bridge. This model will be subjected to loads according to the Dutch NEN norms to have a first realistic estimation of the tensile forces that will occur in the connectors. The results from the monitoring at the bridge and the force predictions made by the model will be compared and used to answer what the short-term and long-term differences in behaviour are between both connectors and answer the research questions.

2. Literature review

The aim of this chapter is to provide knowledge about the use of fibre-reinforced polymer (FRP) bridge decks in bridge engineering. It begins by exploring the motivations for choosing FRP as a material for bridge decks, including its mechanical properties, durability, and advantages over traditional materials such as steel and concrete. Following this, an overview of the various types of FRP bridge deck systems will be presented, highlighting their structural characteristics and typical applications. After this, multiple connection methods will be discussed that are used to connect FRP bridge decks to the supporting superstructure. Finally, the iSRR connector and Lindapter connector, that are used at the Ulsderbrug, will be discussed. The working of both connectors will be described as well as their advantages and disadvantages.

2.1 FRP decks

FRP (Fibre Reinforced Polymer) is an innovative material that is increasingly used as a structural material because it has a high strength-to-weight ratio, good corrosion resistance and is a durable material. Because of these properties, FRP is used as material for bridge decks. These decks can be designed in multiple ways by combining a polymer matrix (like epoxy, polyester, or vinyl ester) with reinforcing fibres (such as glass, carbon, or aramid). The most common FRP decks will be discussed shortly below.

2.1.1 Pultruded FRP Decks

Pultruded decks, are manufactured using a process known as pultrusion, a term derived from "pull" and "extrusion." Pultrusion is a continuous fabrication method where reinforcing fibres are pulled through a resin bath and then through a heated die. Inside the die, the resin cures and the composite takes on its final shape. After exiting the die, the material undergoes post-curing while it continues to be pulled toward a saw, which cuts it into the required length (Eckold, 1994). This process is illustrated in Figure 2.1.

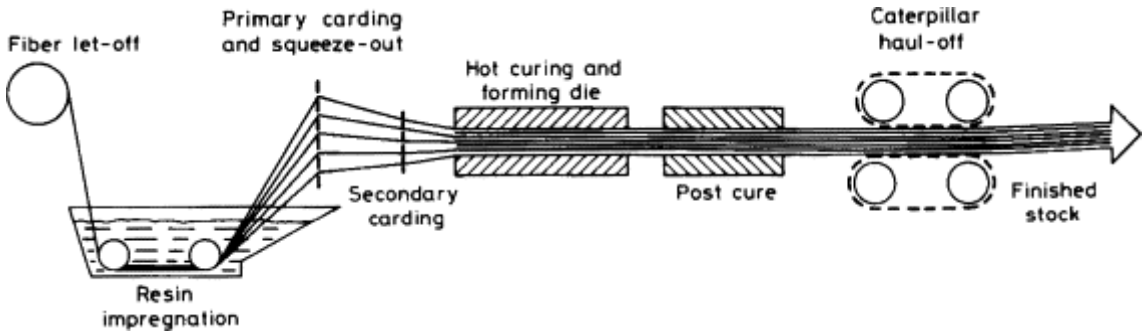

Figure 2.1: Production process pultruded FRP deck (Eckold, 1994)

Pultrusion offers several advantages, including a high stiffness-to-weight and strength-to-weight ratio, precise control over wall thickness, cost efficiency, and suitability for high-volume production. The resulting profiles have constant cross-sections and can take the form of tubes, sheets, or more complex geometries. Examples for pultruded FRP bridge deck can be found in Figure 2.2. The cross-sectional geometry of pultruded bridge decks plays a critical role in their structural performance. These geometries may vary from trapezoidal to triangular shapes. The orientation and angle of the internal webs influence both the local buckling behaviour and the way loads are transferred between the flanges (Thomas Keller, 2006).

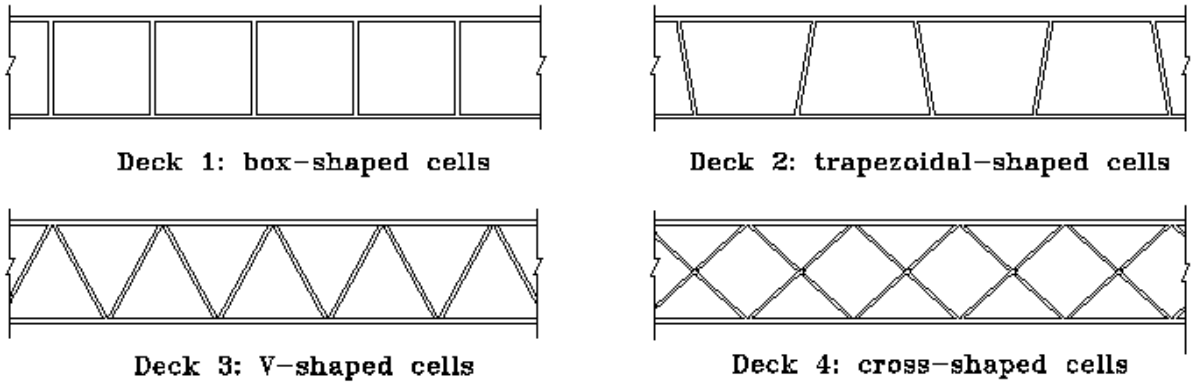

Figure 2.1: Different types of pultruded decks (Zureick, 1995)

2.1.2 Sandwich decks

This type of deck is used at the Ulsderbrug, the bridge that is used for the monitoring. A sandwich deck typically consists of three layers: two outer face sheets (top and bottom) and a core material sandwiched in between. These layers are adhesively bonded together, forming a unified structural component. The face sheets act as the primary load-carrying element. They bear the tensile, compressive and bending stresses. The function of the core is the provide shear resistance and increase the moment of inertia of the deck while minimally adding weight (Avilés, 2008).

Sandwich decks are commonly manufactured using the vacuum infusion process, a composite fabrication method that uses vacuum pressure to draw resin into a dry laminate. In this process, liquid resin is first introduced into a mould cavity, after which vacuum pressure is applied to pull the resin through the reinforcing layers, ensuring thorough impregnation and strong bonding (H. Awais, 2020). The process is illustrated in Figure 2.3.

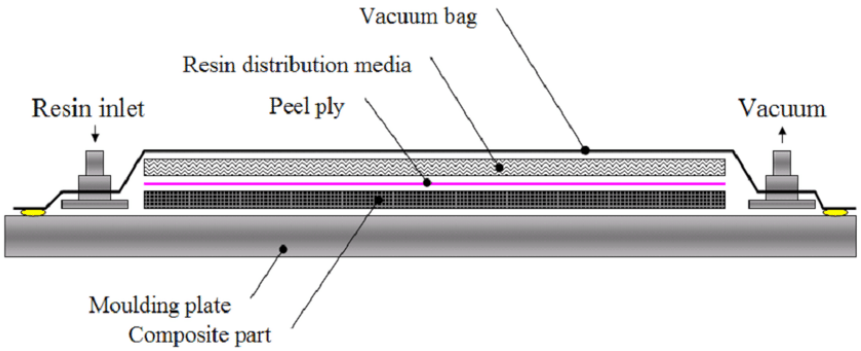

Figure 2.2: Production process of sandwich decks (K. Abdurohman, 2018)

The core of a sandwich deck can be engineered using various materials and configurations, depending on the requirements. Common core types include foam cores, honeycomb cores, and truss cores, as illustrated in Figure 2.4. Each core type offers distinct advantages and limitations.

A honeycomb core (Figure 2.4(b)) consists of a tightly packed array of cells bonded to the face sheets of the sandwich deck. This configuration provides excellent compressive and shear strength while maintaining a low weight. Honeycomb cores can be manufactured from materials such as aluminium or FRP, with customizable cell sizes to meet specific mechanical or structural needs. However, honeycomb cores tend to be relatively expensive and challenging to manufacture, as they require precise bonding to the face sheets to ensure proper structural performance[(Vinson, 2005)].

A truss core (Figure 2.4(c)) is made out of a network of angled struts that directly connect the top and bottom face sheets, forming a load-bearing internal truss. This design offers high shear stiffness and strength. An other advantage is that the truss pattern can be tailored for different load paths or stiffness requirements. However, due to its non-uniform structure, care must be taken to prevent local buckling of the core members. This makes design and analysis more complex compared to more uniform cores like honeycomb or foam (Vinson, 2005).

The sandwich deck at the Ulsderbrug is constructed with a foam core with integrated FRP webs. A foam core (Figure 2.4(a)) provides a high stiffness-to-weight ratio at a relatively low cost. However, foam cores possess limited shear strength. This is why internal FRP webs are integrated within the foam core. These act like embedded I-beams, enhancing both transverse and longitudinal stiffness of the deck. The internal webs also improve load transfer, offer resistance to buckling, and provide additional load paths. Despite these enhancements, foam cores still offer lower shear performance compared to honeycomb and truss core alternatives.

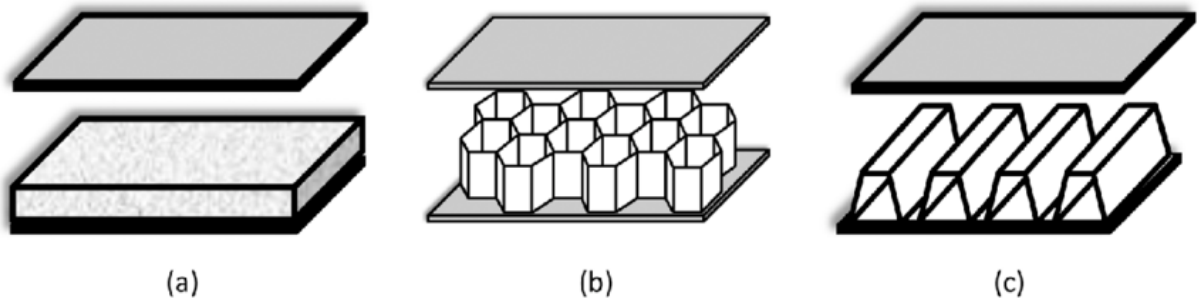

Figure 2.3: Different types of FRP sandwich decks (K. Gunaydin, 2022)

2.2 Connection methods for FRP decks

There are several methods to connect a FRP bridge deck to the steel superstructure of the bridge. The most common methods will be shortly described below.

2.2.1 Adhesive connectors

The first connection method considered is adhesive bonding, in which the FRP bridge deck is bonded to the steel girders using a structural adhesive. These adhesives are typically epoxy-based or polyurethane-based and are applied along the contact interface between the deck and the girder.

One of the main advantages of adhesive bonding is that it does not require drilling or bolting into either the FRP deck or the steel girder flange. This avoids stress concentrations and minimizes damage to structural components. Additionally, adhesive connections simplify installation and generally offer better fatigue performance under cyclic loading compared to mechanical connectors (X. Jiang, 2012).

However, adhesive bonding also has some limitations. Its performance can degrade under extreme temperatures or high humidity, which affects long-term durability. Moreover, quality control during on-site application is challenging, and loads cannot be applied until the adhesive has fully cured. For these reasons, adhesive connections are often used in conjunction with mechanical fasteners to provide redundancy and enhance reliability (Landrock, 2009).

2.2.2 Bolted connectors

Bolted connections are a commonly used mechanical fastening method to join FRP bridge decks to steel superstructures. In this approach, steel bolts pass through both the FRP deck and the flange of the steel girder, often with washers and nuts on either side to secure the assembly. This category of connections can be subdivided into traditional bolts and blind bolts. First traditional bolts will be shortly discussed, blind bolted connectors will be discussed in the next section.

Due to practical reasons, traditional bolts can only be used having a long shaft penetrating the entire depth of the deck and flange of the girder. This is illustrated in Figure 2.5. Using shorter shafts which only penetrate the bottom FRP facing and girder flange, is not practical since the nut or bolt head inside the panel core cannot be accessed after the production.

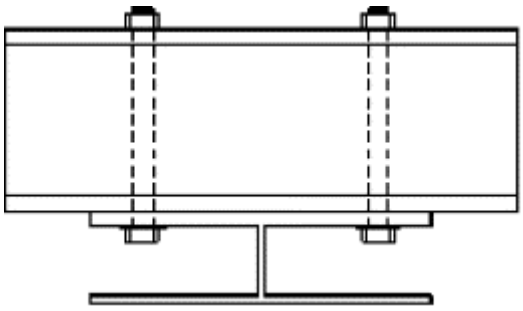

Figure 2.4: Bolted connector for FRP deck (K. Park, 2006)

2.2.3 Blind bolted connectors

Blind bolts are bolts that only require one side of access. They are more frequently used as deck-to-girder connections because they can be easily installed in pre-drilled holes from underneath the bridge. In this section three blind bolted connectors will be discussed. First the Ajax connector will be discussed, then the Lindapter connector and finally the iSRR connector which will be discussed. The latter two blind bolted connectors are the connectors that are monitored at the Ulsderbrug. After the working of the three blind bolted connectors has been explained, the three connectors will be compared.

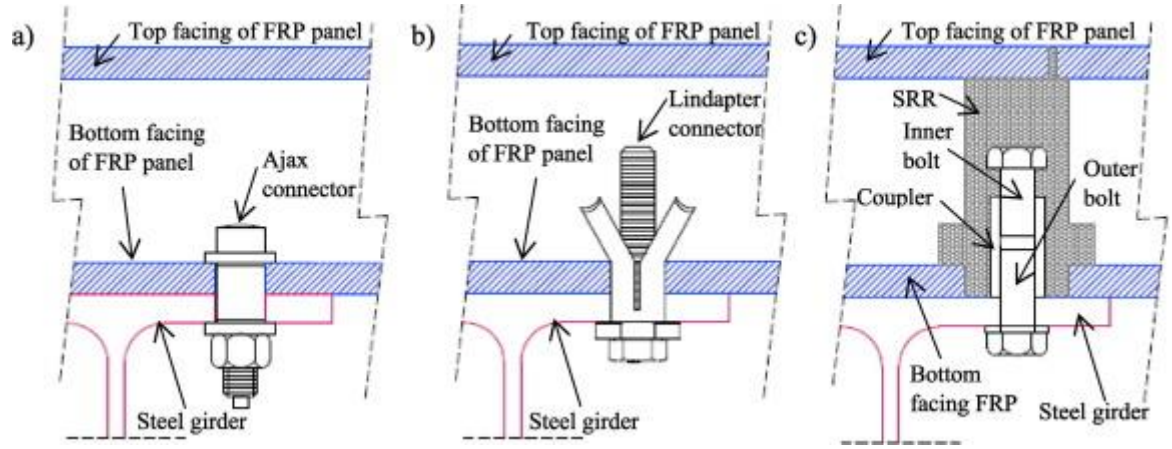

Figure 2.5: Blind-bolted connectors for FRP bridge deck-girder connection (a) Ajax, (b) Lindapter, (c) iSRR (F. Csillag, 2021)

2.2.3.1 Ajax connector

The first blind-bolted connector that will be discussed is the Ajax connector, shown in Figure 2.6(a). The connector can be installed from one side through predrilled holes and is also removable if necessary. The connector is secured by a foldable washer on the embedded end of the bolt, while a standard washer is used on the accessible side.

2.2.3.2 Lindapter connector

The first of the two connectors that has been applied at the Ulsderbrug is the Lindapter bolted connector. This connector is displayed in Figure 2.6 (b) and Figure 2.7, requires predrilled holes and is removable if needed. This blind-bolted connector uses a sleeve expansion mechanism inside a hollow section, in this case the bridge deck. The tightening of the bolt forces the sleeve to expand outward, clamping against the wall of the hollow section. This creates a secure clamping force. (G. Olivier, 2023) investigated both experimentally and numerically the static shear resistance of two blind bolt connectors, i.e. M20 8.8 Ajax and Lindapter system. Five push-out tests concluded that the Ajax and Lindapter system provide good ductility (20 mm) due to excessive bearing damage and yielding of the bolts.

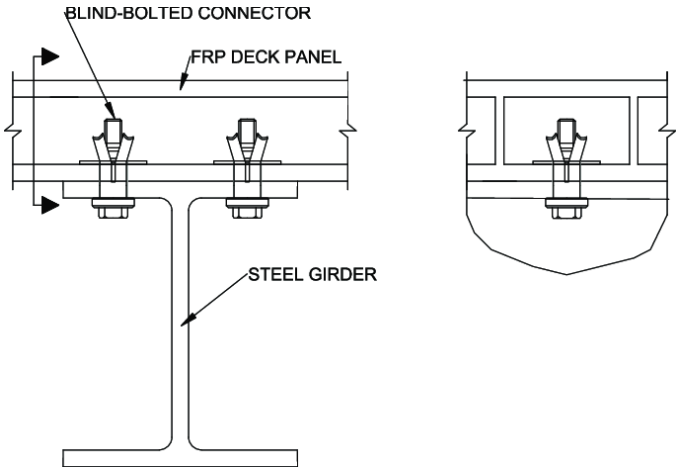

Figure 2.6: Lindapter bolted connector connecting FRP bridge deck to steel girder (G. Olivier, 2023)

In the push-out test, eight specimens were examined. The Ajax and Lindapter shear connectors failed due to laminate crushing combined with bolt yielding, and bearing failure damage was observed in the FRP laminate. The average shear resistance for the Ajax and Lindapter connectors was 207.4 kN and 164.3 kN, respectively. In contrast, the iSRR connector exhibited a brittle failure mode characterized by bolt fracture. Minimal damage to the FRP deck indicated potential for structural component reuse, with an average shear resistance measured at 120 kN.

2.2.4 iSRR connector

The second connector type that connects the FRP bridge deck to the superstructure at the monitored bridge is the iSRR connector. The iSRR (injected Steel Reinforced Resin) connector is an innovative system currently under development at TU Delft, designed to address a key challenge in the full-scale adoption of hybrid steel-FRP (Fibre Reinforced Polymer) bridges. Its primary objective is to enable demountable connections that support full composite action between steel girders and FRP bridge decks. The core of the iSRR system is the use of Steel Reinforced Resin, a composite filler material. The process involves filling the drilled bolt holes with steel shot balls, which are then bonded together by injecting resin into the remaining voids. The resin is essential to prevent rigid body displacement of the steel balls and to ensure the structural integrity of the connector (Figure 2.6(c)).

The iSRR connector combines the principles of resin-injected bolts and blind bolts. The iSRR connector can both be installed on-site or be prefabricated at another location (Figure 2.8 (a) and (b) respectively). When installing the iSRR bolts on site, the bolts are first preloaded on the steel girder. Afterwards the bridge deck is placed on top of the girders and finally the cavities are injected to connect the iSRR bolts to the bridge deck. When prefabricating, the bolts are pre-installed into the FRP deck. During on-site installation, the deck is positioned onto the steel girders, and the bolts are secured by simply tightening the nuts from the underside. The connector is then preloaded to further reduce slip at the steel interface. The combination of a resin injection, to eliminate movement within the FRP deck, and preloading, to minimize slip at the girder, results in an efficient, slip-resistant connector.

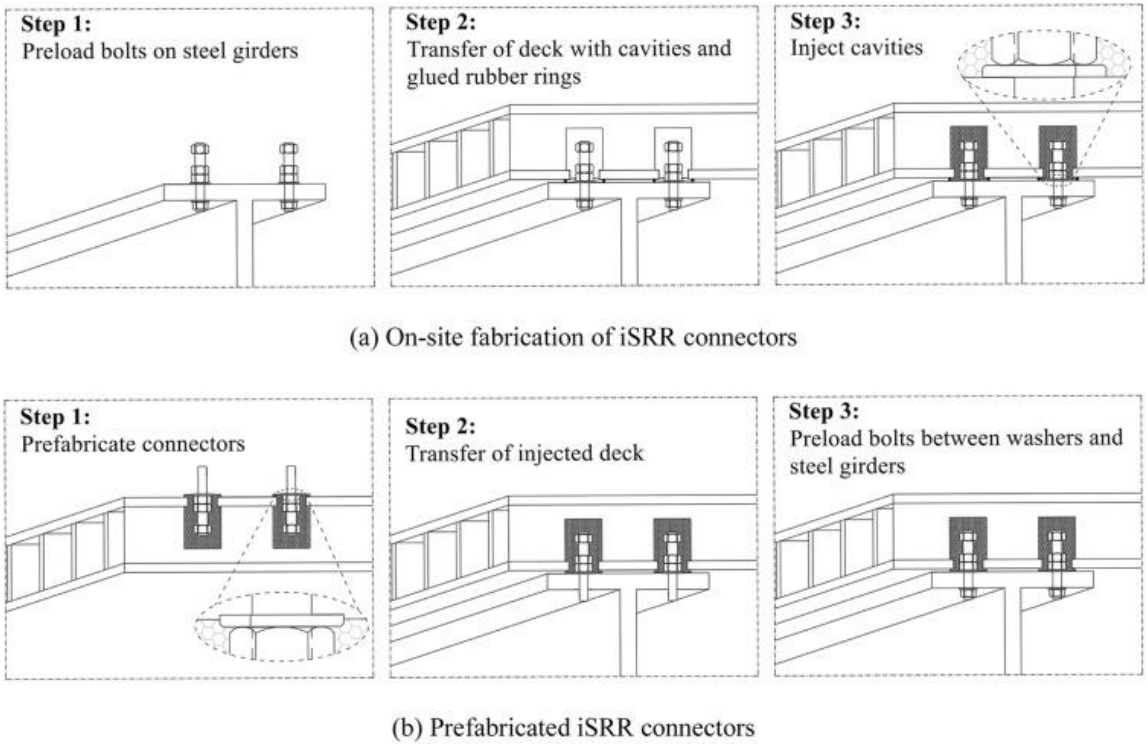

Figure 2.7: Installation process of iSRR connectors both on-site (a) and off-site (b) (A. Christoforidou, 2024)

The concept of using steel-reinforced resin (SRR) was first introduced by M. P. Nijgh who conducted double lap shear tests using steel and various types of resin-injected bolts. The results demonstrated that SRR connectors exhibited 1.5 to 2 times higher stiffness and approximately 40% less creep deformation compared to conventional resin-injected connections without steel shot reinforcement (Nijgh, 2017). Nijgh recommended exploring the application of SRR in other types of connections, particularly those involving oversized holes, which led to its proposed use in FRP–steel connections to mitigate stress concentrations in the FRP facings.

Building on this foundation, Csillag and Olivier and Csillag investigated the structural performance of the iSRR (improved Steel-Reinforced Resin) connectors in FRP–steel hybrid joints. Csillag's initial study focused on advancing demountable deck-to-girder connector. It assessed the static, time-independent performance of three different shear connector types, the Ajax and Lindapter and the iSRR connector, through both push-out tests and numerical simulations. The shear connectors achieved resistances between 120 kN and 200 kN, comparable to those of shear stud connectors used in hybrid concrete-steel bridges. Among them, the iSRR connectors exhibited significantly reduced slip displacements under low-cycle loading, particularly in the initial stages of testing, indicating strong potential for applications requiring high fatigue resistance (Csillag, 2018).

In a follow-up study, Olivier and Csillag extended the investigation to include the time-dependent behaviour of these connectors, focusing on fatigue and creep. They conducted single-lap shear tests on three connector types: Lindapter, iSRR, and conventional injected bolts. The findings revealed that the iSRR connectors outperformed the others, offering superior structural performance across both static and time-dependent loading conditions (G. Olivier, 2023).

3. Bridge monitoring

In this chapter will be explained how the collecting of the data will take place at the bridge. It starts with a discussion of the bridge's structural characteristics, followed by showing how the forces will be measured in the bolts. Following this, the monitoring setup will be described in detail. Finally, the chapter concludes with an overview of the configuration settings of the monitoring system.

3.1 Bridge characteristics

The characteristics of the bridge are examined across five subsections. First, the superstructure of the bridge will be discussed, starting with an overview of the bridge layout, detailing its dimensions and showing how the superstructure is supported. Following this, the composition of the bridge deck will be discussed, showing how the deck is built up and how it is connected to the rest of the bridge. Following, the two types of connectors used in the bridge will be described in detail. Finally, the preloading of the bolts will be discussed.

3.1.1 Superstructure of the bridge

The superstructure of the bridge has been made out of steel and comprises two longitudinal and five transverse crossbeams. The girders run parallel to the length of the bridge, while the crossbeams are orientated perpendicularly and are rigidly connected to the girders at both ends. The bridge has a span of over 13 metres and has a width of more than 7 metres. The exact dimensions and positioning of the structural elements are illustrated in Figure 3.1. The longitudinal girders are simply supported at both ends and maintain a constant cross-section along their entire length. The girders consist of HEA profiles with a height of 911 mm and a width of 418.5 mm. In contrast to the longitudinal girders, the dimensions of the crossbeams differ over the length of the beam. The crossbeams also consist of HEA profiles, but the height of each crossbeam is inclined slightly. The height of the crossbeam at both ends is 590 mm, while the crossbeam has a height of 645 mm at midpoint. The width of the crossbeams is constant, with a width of 450 mm. Exact dimensions of both HEA profiles can be found in Annex A.

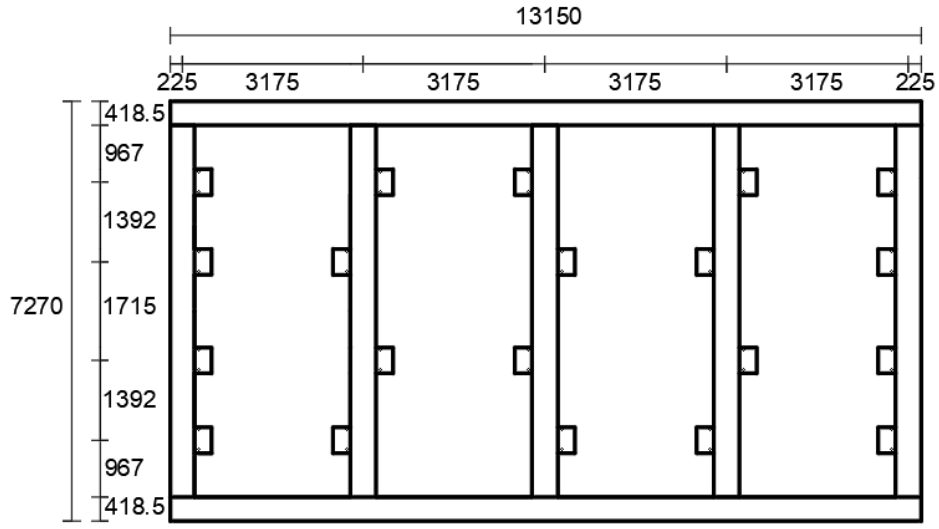

Figure 3.1: Dimensions of the superstructure of the bridge

Figure 3.1 also illustrates the clamping plates that connect the crossbeams to the bridge deck. The spacing between these clamping plates varies over the length of each crossbeam and is indicated in the same Figure. Each clamping plate is mechanically connected to the bridge deck using bolted connectors. The plates have a thickness of 10 mm, while their other dimensions are shown in Figure 3.2. This Figure presents a bottom view of the clamping plate, indicating the positions of the two bolts and showing as well what part of the clamping plate is connected to the flange of the crossbeam. A side view of the clamping plate can be seen in Figure 3.4 in section 3.1.3.

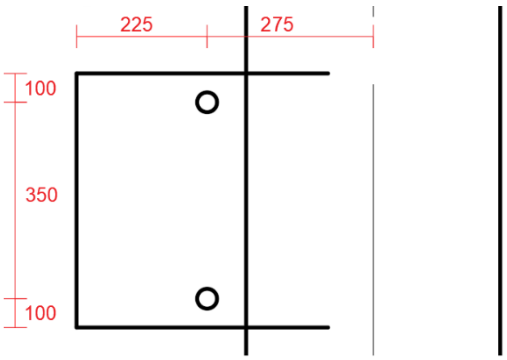

Figure 3.2: Dimensions of the clamping plate

3.1.2 FRP bridge deck

The FRP bridge deck has been designed by FiberCore Europe, a well-known FRP deck producer, and can structurally be seen as a sandwich construction composed of three layers. This is displayed in Figure 3.3. The deck has a total thickness of 288 mm. The core has a thickness of 246 mm while both the top and bottom face sheets have a thickness of 21 mm. The bottom and top layers are made of glass fibre-reinforced polyester (GFRP). In between these face sheets is a shear-rigid, fibre-reinforced core. The top skin, bottom skin, and webs are monolithically connected by continuous fibre reinforcement. The core is made of web plates that connect the upper and lower layers of the bridge. These web plates transfer the shear forces to the supports. The rest of the middle layer consists of foam, which is mainly used for manufacturing purposes.

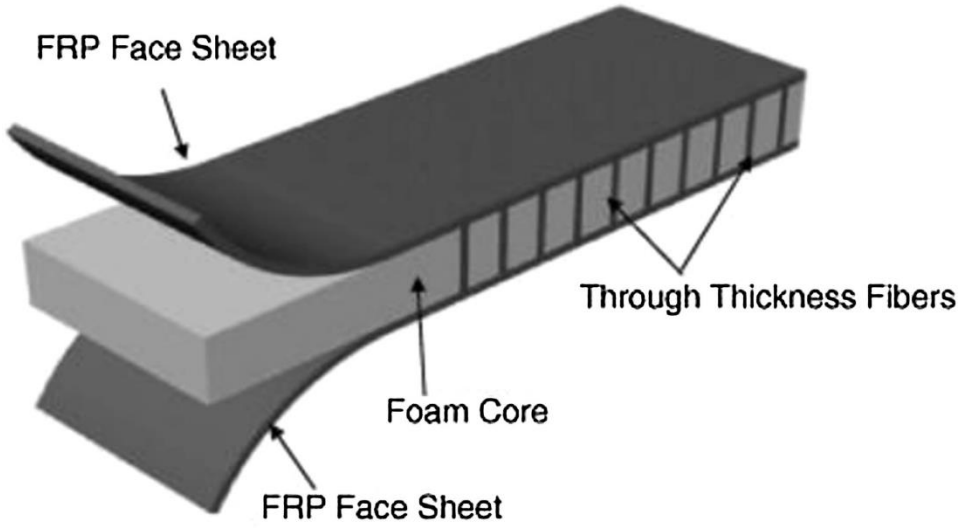

Figure 3.38: FRP sandwich bridge deck with through thickness fibers (A. Manalo, 2016)

The stacking sequence of the laminates of the GFRP bridge deck can be found in table 3.1 for both the facings and the web of the deck (A. Christoforidou, 2024). Different laminates are used, each with its own specific composition and properties. The properties of the laminates are based on the fibre and resin values specified in CUR-aanbeveling 96 and are determined using standard micromechanical and classical laminate theory.

Table 3.1: Stacking sequence of the laminates of the bridge deck

Facings	[45/-45/45/-45/45/-45/0/90/45/-45/0/90/45/-45/90_3/0/90/45/-45/90_3/0/90/45/-45/90_3/0/90/45/-45/90_3/0/90/45/-45]
Web	[-45/45/-45/45/-45/45/-45/45/90/0/-45/45/-45/45/-45/45]

3.1.3 iSRR connector

The iSSR connector is connected to the bridge's crossbeam using a clamping plate, as illustrated in Figure 3.4. Due to this design, the connector is only able to transfer tensile forces. At the core of the connector is an embedded M16 bolt, surrounded by a cavity filled with steel-reinforced resin (SRR) material. This embedded bolt is connected to the external bolt via an M16 coupling nut. Both the embedded and external bolts used in the connector are M16 bolts of strength class 8.8, galvanised, and manufactured to ISO fit standards. The bolts are preloaded with a force of 35 kN.

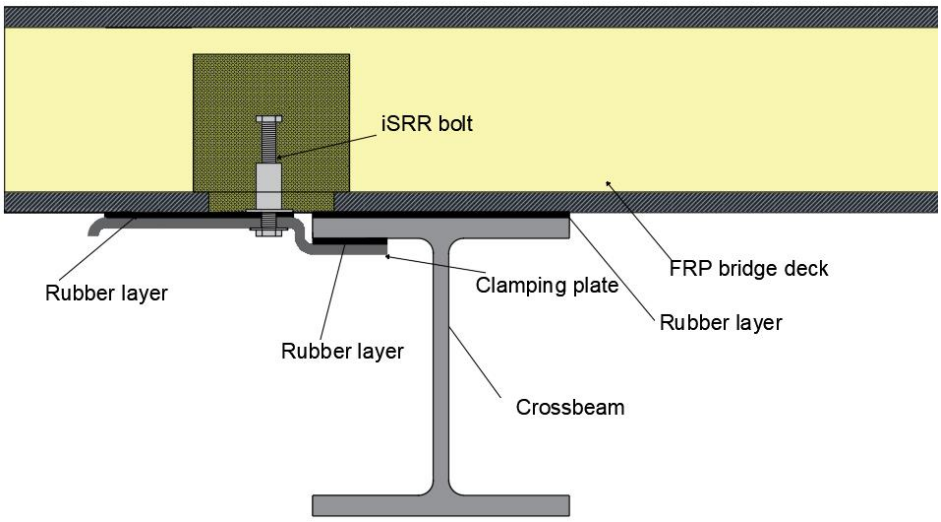

Figure 3.4: iSRR connector

While all embedded bolts have a length of 50 mm, this length is not constant for the external bolts. The external bolt originally had a length of 35 mm, as shown in Figure 3.8. However, for the bolts that are instrumented with strain gauges to monitor the bolt forces, the length of the external bolts has been increased to 80 mm. The length has been increased because the strain gauges required a longer bolt. This new situation is illustrated in Figure 3.9. This modification is discussed in greater detail in Section 3.2.

There are three rubber layers positioned near the connector, as shown in Figure 3.4. The first layer is placed between the clamping plate and the bridge deck, the second between the clamping plate and the crossbeam, and the third between the crossbeam and the bridge deck. These rubber layers, each approximately 10 mm thick, serve to distribute the forces more evenly and cope with imperfections. This prevents the development of stress concentrations. The rubber interlayers also help with the reduction of sound caused by the traffic passing the bridge.

3.1.4 Lindapter Hollo bolt connector

The Lindapter Hollo bolt connector is attached to the bridge's superstructure in the same manner as the iSRR connector by using a clamping plate. This clamping plate follows the same design, which means that this connector is also only able to transfer tensile forces. The bolt used in the Lindapter Hollo bolt connector is an M16 bolt with a length of 100 mm. As with the iSRR connector, bolts of strength class 8.8, galvanised, and manufactured to ISO fit standards have been used. Each bolt is preloaded with a force of 35 kN, the same as for the iSRR connector.

Consistent with the iSRR connector, three rubber layers are positioned near the connector, as illustrated in Figure 3.5. These layers are arranged in the same locations and have an approximate thickness of 10 mm. Their purpose is the same, they distribute loads, reduce stress concentrations and reduce the sound caused by vehicles driving over the bridge.

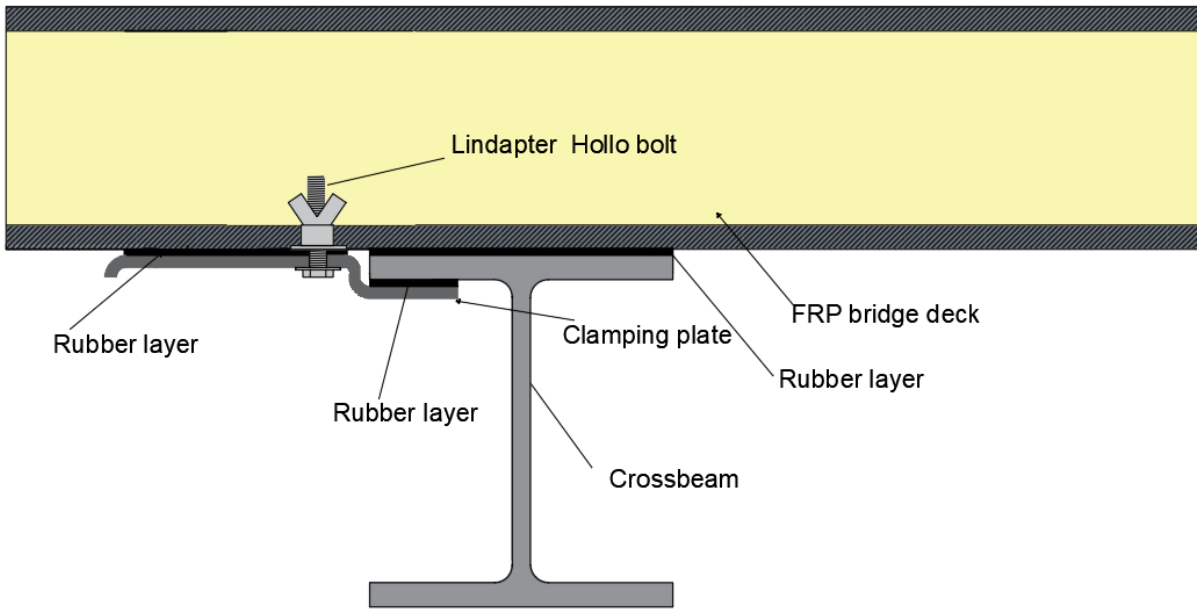

Figure 3.5: Lindapter Hollo bolt connector

3.1.5 Preloading of the bolts

The bolts of both types of connectors are being preloaded with a preloading force of 35 kN. The effect of preloading the bolts will be discussed shortly below. Figure 3.6 shows the preloading at the bolt of a Lindapter connector. The preloading for the iSRR connector works in the same way. The rubber interlayers have been left out of this Figure to make the effects of preloading better visible. In this Figure, the red arrows show the preloading of the bolt while the blue arrows display the locations where contact pressure is added between the bridge elements. Adding contact pressure is beneficial for the distribution of the transferred loads and reduces stress concentrations. The preloading of the bolts adds contact pressure at three different locations at the connector. Namely, between the bridge deck and the cross beam, between the bridge deck and the clamping plate and between the clamping plate and the cross beam. It is important to have a sufficient preloading force present at all connectors. The loss of preload, which is displayed in Figure 3.7 for a Lindapter connector, could lead to a decrease in contact pressure between the bridge elements. This is illustrated by the blue arrows in this Figure. This is especially relevant for the contact between the clamping plate and the cross beam of the bridge, where gravity does not assist with maintaining contact pressure. The contact pressure could get loose at this location, which could lead to a worse distribution of forces and increased stress concentrations.

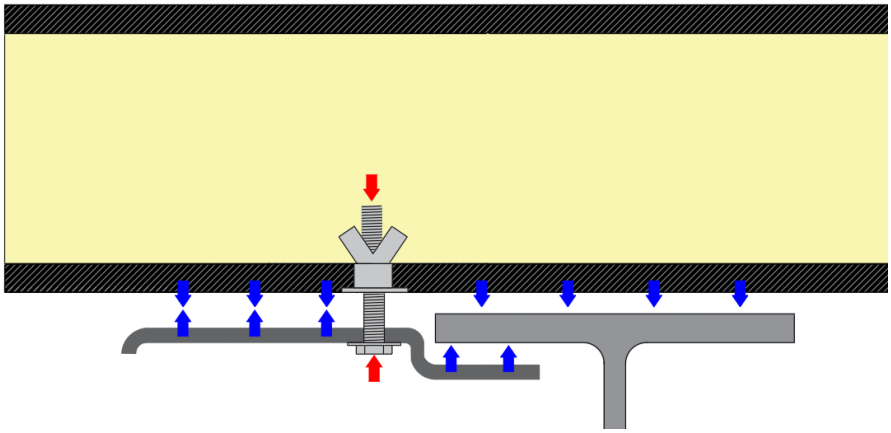

Figure 3.6: Effect of preloading the bolts for the Lindapter connector

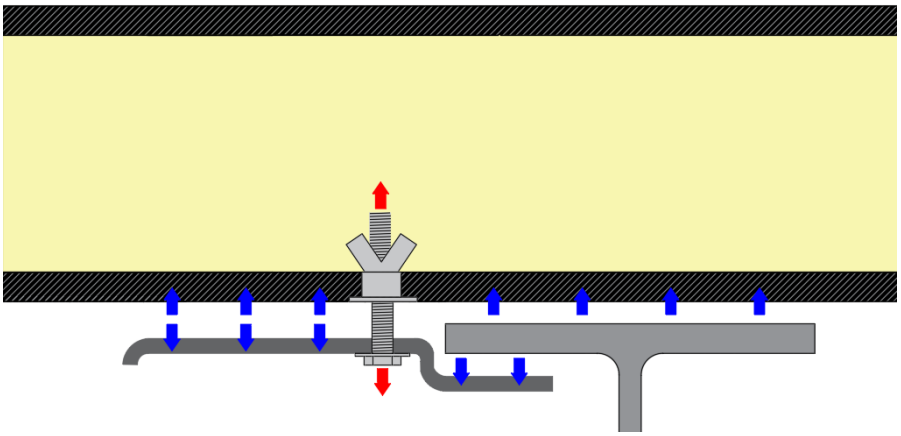

Figure 3.7: Loss of preload at Lindapter connector

3.2 Measurement of bolt forces

The forces in the bolts will be monitored by strain gauges fitted in the bolts. The strain gauges will be connected by cables to the box in the tower of the bridge. Strain gauges were chosen because they are a reliable way of measuring the forces, and they are also cheaper and ready for use faster than measuring rings for the bolts. Nine bolts with strain gauges will be prepared and tested in the Stevin II lab of TU Delft. Eight of these will replace the existing bolts in the bridge for monitoring, and the ninth will serve as a dummy.

In order to place the strain gauges in the bolts, holes must be made in the bolts. For the Lindapter Hollo bolt connector this is not a problem because the bolt has sufficient length, but because the length of the currently used bolts of the iSRR connector of 35 millimetres is insufficient for the strain gauges, these bolts will be replaced by longer bolts with a total length of 80 mm (see Figures 3.8 and 3.9). The depth of the bolt hole in the iSRR connector is 50 mm, which is less than the length of the bolt. To compensate for this difference and ensure proper installation, M16 washers will be used to achieve the required bolt fit.

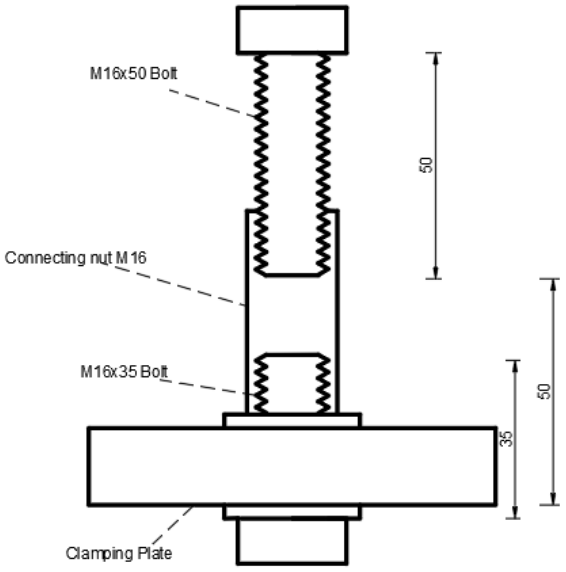

Figure 3.89: Original situation iSRR connector

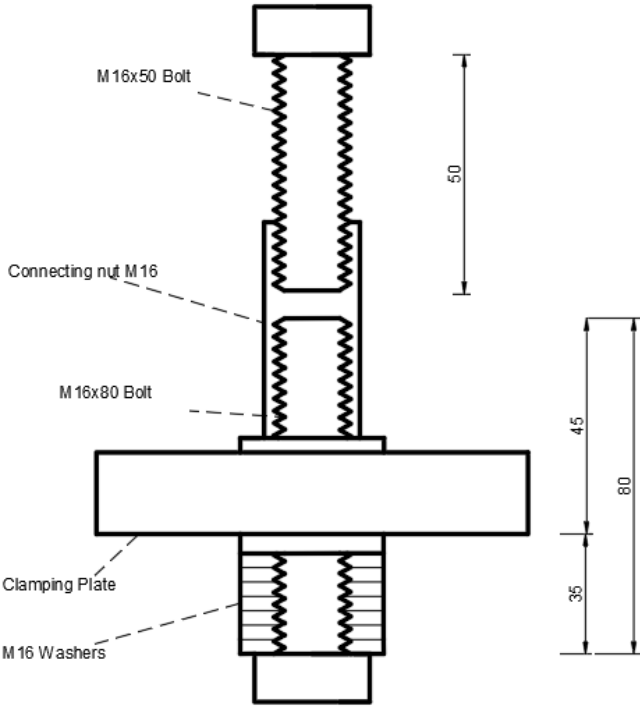

Figure 3.910: Adjusted situation iSRR connector

In order to be able to fit these strain gauges into the bolts, holes of 40 millimetres long with a diameter of 2 millimetres were made by means of spark erosion. This can be seen in Figures 3.10 and 3.11 for both types of bolts. This length of 40 millimetres is the minimum length for this type of strain gauge and ensures that the measured forces in the bolt are not influenced by the head of the bolt. After making and cleaning the holes, the strain gauge will be placed. This is done by filling the hole with a special glue and then placing the strain gauge in the desired position. The strain gauges will be connected to the head of the bolt with two copper wires, these wires will transmit the forces to the monitoring system. After a day of drying, the bolts are ready for use and can be calibrated. Finally, the bolts are tested together with the measuring system to see if everything works and the software is set up correctly.

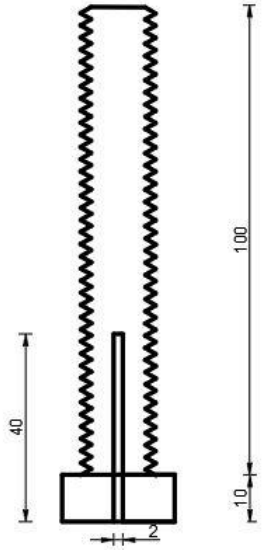

Figure 3.10: Strain gauge Lindapter Hollo bolt

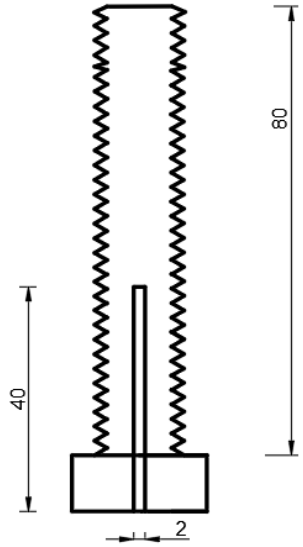

Figure 3.11: Strain gauge iSRR bolt

When installing the strain gauge at the connector, it is important to make sure that the strain gauge is located within the clamping package of the connector. This is necessary for the correct measurement of the forces. The clamping package for the Lindapter connector consists of the washer, the clamping plate and the rubber interlayer. Figure 3.12 shows that the installed strain gauge is located within this clamping package. The clamping package for the iSRR connector is shown in Figure 3.13. The clamping package differs from the Lindapter connector. The difference is due to the addition of washers used to compensate for the increased bolt length in the iSRR connector. The clamping package consists of the 11 added washers, the initial washer, the clamping plate and the rubber interlayer. The strain gauge is located within this clamping package, so that the forces will be measured correctly.

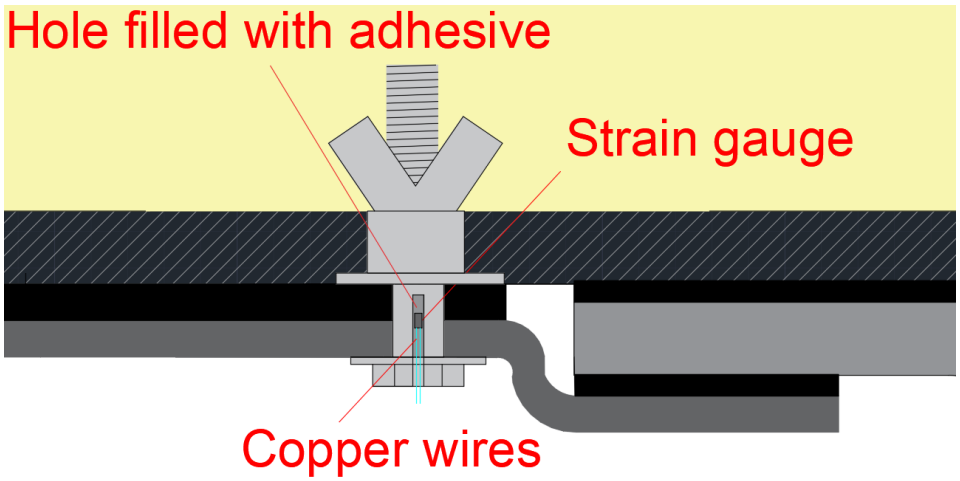

Figure 3.1211: Strain gauge installed at the Lindapter connector

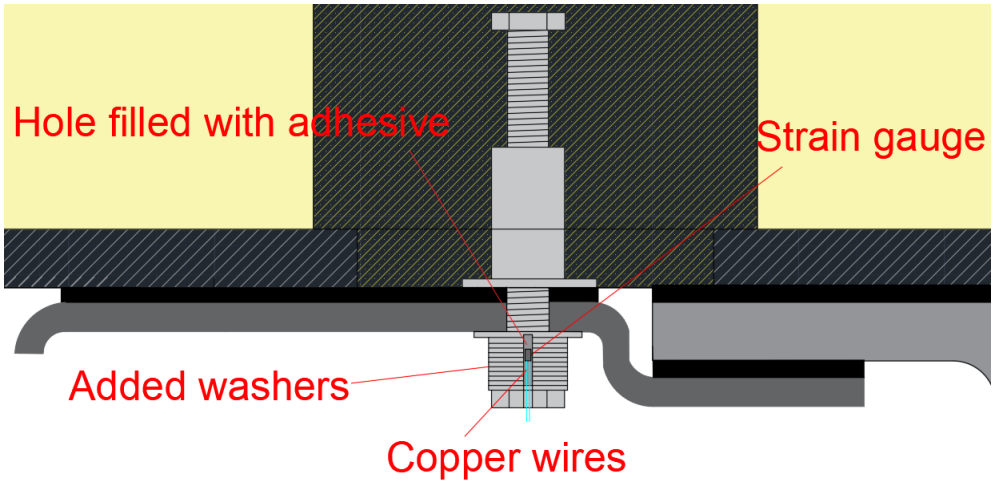

Figure 3.1312: Strain gauge installed at the iSRR connector

3.3 Monitoring set up at the bridge

To enable the measurement of forces in the bolts, a monitoring system was designed and constructed at the Stevin II laboratory of TU Delft. This system records the bolt forces in four iSRR connectors, four Lindapter Hollo bolt connectors, as well as the temperature. Additionally, one dummy sensor is included to allow for noise filtering, if necessary.

The monitoring system comprises various components housed within an enclosure that will be installed in the tower of the bridge. This location provides a degree of protection from environmental conditions and moisture, and also allows for a reliable power supply. The enclosure is equipped with ventilation to prevent overheating during warmer days. Heating for winter conditions is not required, as the system itself generates sufficient heat during operation.

Cables from the bolts are connected externally to the enclosure and routed to the data acquisition board inside. The measurement data are transmitted from the acquisition board to a computer located within the enclosure. A modem enables remote access to the computer, allowing for data transmission, storage, and processing to be done remotely. The modem's antenna is mounted on the exterior of the tower to ensure signal reception.

The internal configuration of the enclosure is shown in Figure 3.14. On the right-hand wall of the enclosure, ten connection ports for the sensor cables are visible. From these ports, the cables are routed to the data acquisition board located centrally within the enclosure, which is in turn connected to the computer on the left-hand side. The modem is situated in the lower right corner, with cables running through the right wall to connect to the external antenna. The ventilation fan, located in the lower left corner, is positioned at the opposite side of the box than the ventilation opening to ensure effective airflow throughout the entire enclosure.

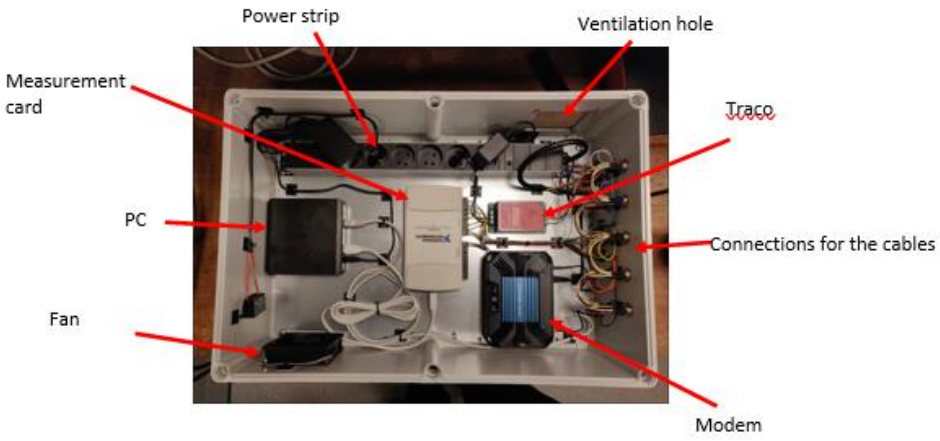

Figure 3.14: Measurement system

3.4 Measurement settings

The monitoring system has been designed in such a way that it can be operated remotely, and measurement data can be accessed and downloaded from a distance. Several configurations have been implemented for the measurements; below is a brief summary of what is being measured and how the system has been set up.

The first parameter measured is the average bolt force in all eight bolts. The force in the bolts is recorded every 30 seconds to ensure that the effects of traffic loads are not captured. This measurement runs continuously, 24 hours a day, and will be used to assess preload loss and the influence of temperature on bolt forces.

The second measurement records the peaks and troughs in bolt forces caused by traffic loads. This measurement also operates continuously and is used to determine the volume of traffic and the resulting load cycles in the bolts.

The third type of measurement involves high-frequency sampling of the bolt forces, recorded every 0.02 seconds. This measurement is conducted for one hour per day—during the morning rush hour—in order to capture as many traffic-induced loadings as possible without generating excessively large data files. The results from this measurement will be used to analyse short- and long-term load cycles caused by traffic.

In addition, temperature is measured continuously, 24 hours a day, just beneath the bridge. For wind load data, which is necessary to assess the effects of bridge opening and closing, meteorological data from the KNMI (Royal Netherlands Meteorological Institute) will be used.

4. Results

In this chapter the results of the monitoring will be discussed. First, will be explained how a controlled truck load has been applied at the bridge. After this, the short-term behaviour of both connectors due to traffic loading and opening of the bridge will be discussed. Followed by the impact of temperature on the bolt forces and the loss of preload. Finally, the long-term behaviour of the connectors will be discussed.

4.1 Traffic loading

To assess the sensitivity of the system to both types of connectors, the response to short-term traffic loads will be examined on-site. To interpret the measurement results correctly, a reference measurement was conducted with a known vehicle. This known vehicle is a four-axle truck with a known weight. This reference measurement was performed for four different speeds, keeping the load on the bridge constant. Since these measurements were taken at the time when the preload force in the bolts was reapplied, the traffic load was applied both before and after reapplying the preload force. This allows for an examination of the influence of the preload force in the bolts on the response to traffic loads and conclusions to be drawn regarding how this affects the forces in the bolts. In this chapter, the applied load will be discussed first. Secondly, the influence of the velocity of the truck on the forces in the bolts will be looked at. After this, the responses of the Hollo bolts and iSRR bolts will be examined respectively. Afterwards, these responses will be compared for both types of connectors.

4.1.1 Vehicle load

Figure 4.1 illustrates the schematisation of the wheel load and the location of the reference load. In this Figure, the load is shown on the right side. This load consists of eight contact points since the truck has four axles. Each contact point with the bridge is indicated as a red square measuring 0.4 by 0.4 meters in the Figure below, the area used for truck loads in the Eurocode, with the corresponding distance between them. According to the green line, this load will drive over the bridge at different velocities and will reverse back over the bridge at a walking pace along the same route. This distance from the bolts to the applied load is therefore constant for each passage. The weight of the truck was measured shortly before the measurement; the truck has a mass of 26,040 kg. A picture of the truck and the weighing can be found in Appendix 1.

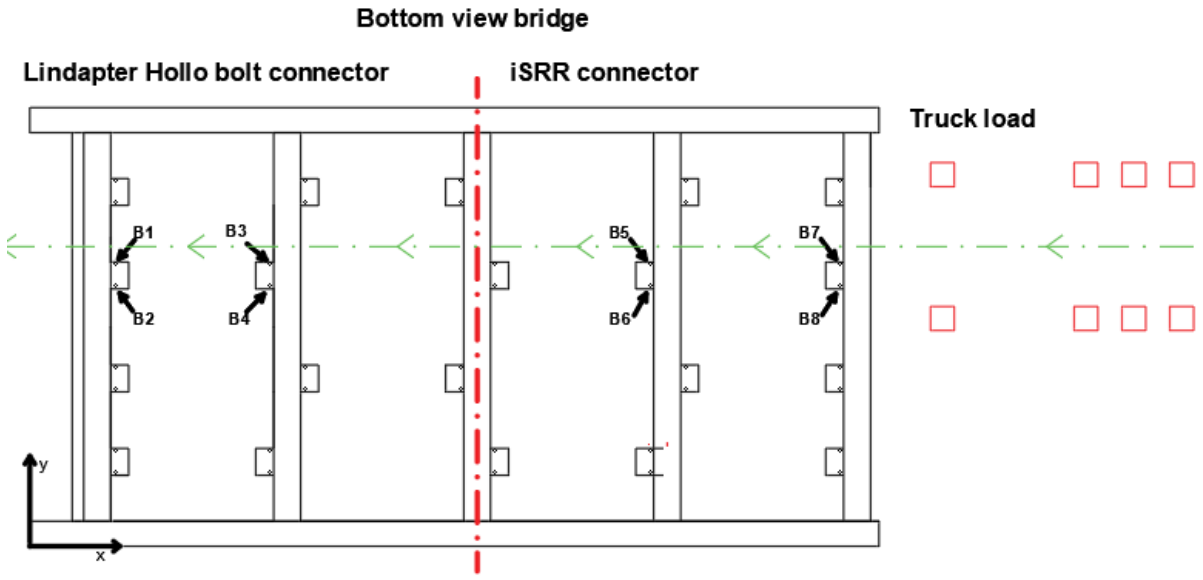

Figure 4.113: Path of truck load over the bridge

4.1.2 Influence of the velocity of the truck

To observe the influence of the truck's speed on the forces in the bolts, the truck drives over the bridge at various speeds. This is done at a walking pace and at 10, 20 and 30 km per hour. The resulting forces for Hollo bolt 2 are indicated in Figures 4.2 and 4.3. The forces resulting from the different speeds of the truck for iSRR bolt 5 are shown in Figure 4.4 and 4.5. These two bolts were chosen to represent the response to different speeds for both types of connectors because they have the clearest response. The other bolts react in a similar manner and with a similar magnitude as bolt 5.

From Figure 4.2 and 4.3, it can be concluded that for the Hollo bolts, both before and after reapplying the preload force to the bolts, the different speeds of the truck result in a response with nearly identical magnitude. The difference in magnitude is less than 0.05 kN Therefore, it can be concluded, that the speed at which the truck travels over the bridge as almost no effect on the magnitude of the force in Hollo bolt 2. However, the bolt is subjected to a longer load than a walking pace load because the truck remains on the bridge for longer.

For iSRR bolt 5, in Figures 4.4 and 4.5, reactions of similar magnitude are observed for the different speeds of the truck. The difference in reaction magnitude is, just like for the Hollo bolt 2, smaller than 0.05 kN. This is relatively small compared to the force in the bolt.

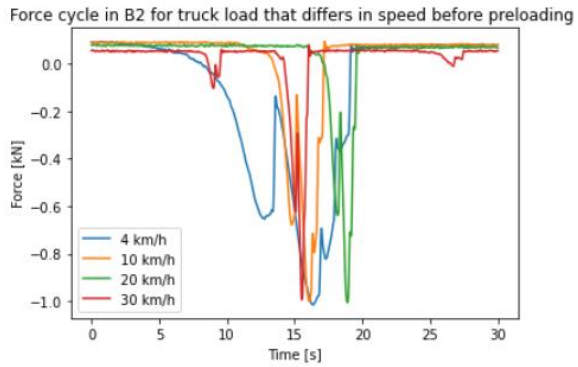

Figure 4.214: Force cycle for iSRR bolt for different velocities of truck before preloading

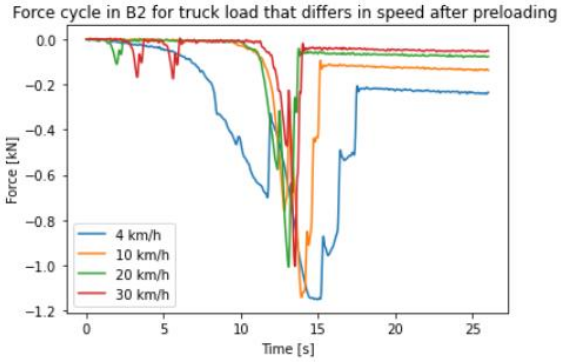

Figure 4.3: Force cycle of iSRR bolt for different velocities of truck after preloading

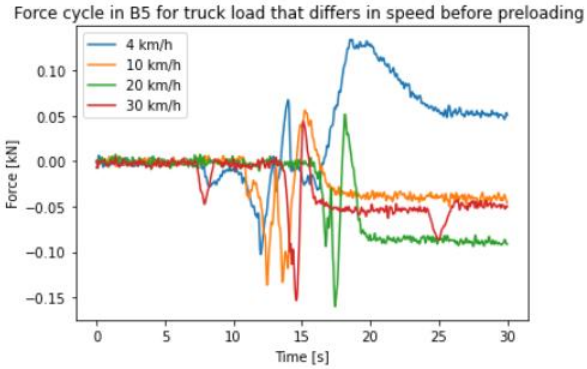

Figure 4.415: Force cycle in Lindapter Hollo bolt for different velocities of truck before preloading

Figure 4.516: Force cycle in Lindapter Hollo bolt for different velocities of truck after preloading

4.1.3 Lindapter Hollo bolt connector

To compare the responses of the Lindapter Hollo bolts, the bolt forces before and after re-preloading are presented in Figures 4.6 and 4.7. These responses correspond to the truck moving slowly across the bridge. The bolt forces are shown as percentages in the Figures to facilitate comparison among the different bolts. The responses of all bolts at other truck speeds can be found in Appendix 3.

The Figures below show that the shape of the response curves of all bolts to the truck loading is nearly identical both before and after re-preloading. The magnitude of the bolt responses also remains the same; the percentages are higher in Figure 4.6 only because the preload force is lower than in Figure 4.7. This means that the magnitude of the preload force in the bolts has little influence on the response of the Lindapter Hollo bolts to the loading caused by the truck. However, Figure 4.7 does show that the force in Bolt 2 does not fully return to 100% of the preloading level. This is due to the fact that the bolt was recently re-preloaded, resulting in a relatively rapid decrease in force at that moment. As previously noted, this rapid loss of pre-tension is a consequence of the rubber interlayer between the bridge deck and the clamping plate.

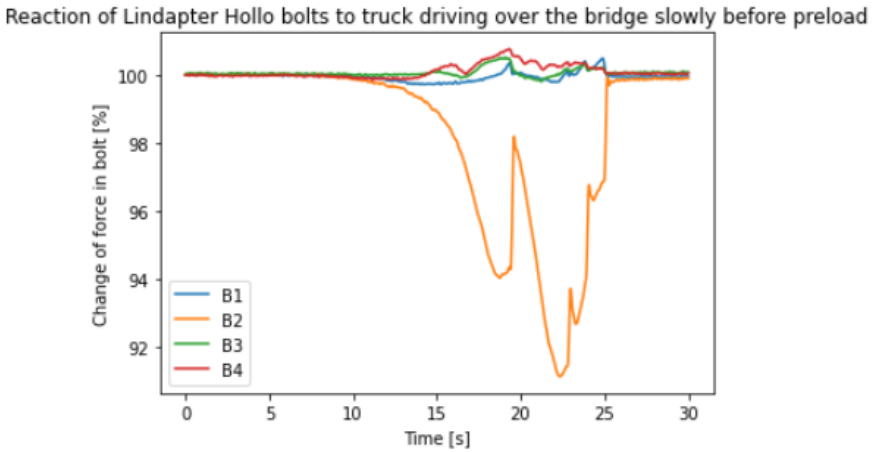

Figure 4.6: Lindapter Hollo bolts under truck load before preload

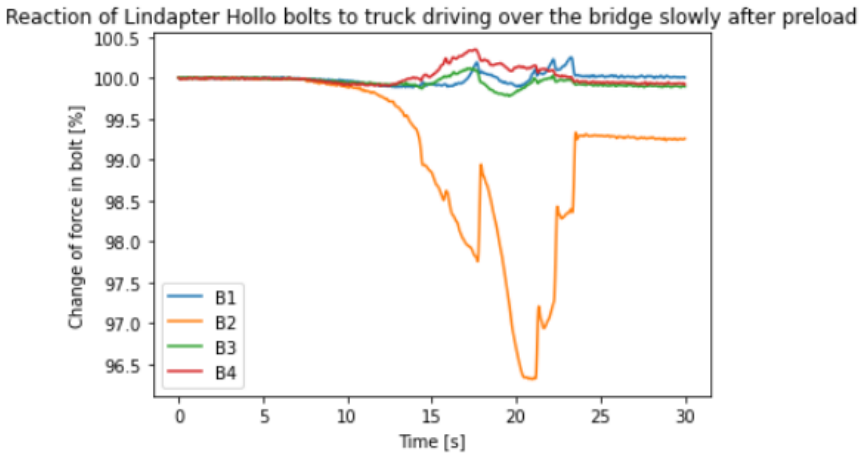

Figure 4.717: Lindapter Hollo bolts under truck load after preload

However, what becomes most evident from Figures 4.6 and 4.7 is that the magnitude of the response of the Lindapter Hollo bolts varies per bolt. It can be observed that bolts 1, 3, and 4 exhibit responses of comparable magnitude, with a force difference of approximately 0.5%, corresponding to about 0.12 kN. The response of bolt 2, however, is with 1.18 kN approximately ten times greater, both before and after reapplying the pre-tension to the Lindapter Hollo bolts.

Differences in response magnitude among the bolts can be attributed to several factors. The first factor is the location of the bolt. Bolts located closer to the load are likely to experience greater responses than the bolts positioned further away. Additionally, small variations in preload, the presence of rubber between the plate and the bridge deck, and the geometry of the clamping plate may also influence the response. Nevertheless, the difference between bolt 2 and the other Lindapter Hollo bolts is so large that it is likely to be caused by another factor. This issue will be addressed in more detail later in this chapter.

4.1.4 iSRR connector

The bolt forces of the iSRR bolts subjected to the truck moving slowly across the bridge are shown in Figures 4.8 and 4.9. Figure 4.8 presents the bolt responses before the pre-tension force was reapplied, while Figure 4.9 shows the responses after reapplication. The forces are expressed as percentages to allow for straightforward comparison.

The magnitude of the response of the iSRR bolts to the loading, both before and after the application of the pre-tension force, does not exceed 1% of the applied pre-tension at the respective moment. This corresponds to force variations of less than 0.2 kN. The differences in the bolt responses are relatively small and are likely due primarily to the location of the bolts and potential imperfections in the connection. These imperfections will be discussed in more detail later in this chapter.

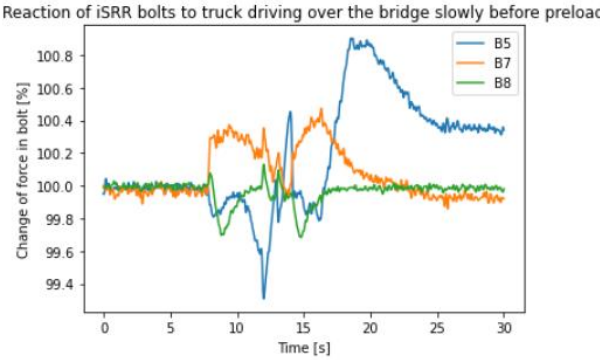

Figure 4.8: Force in iSRR bolts under truck loading before preload

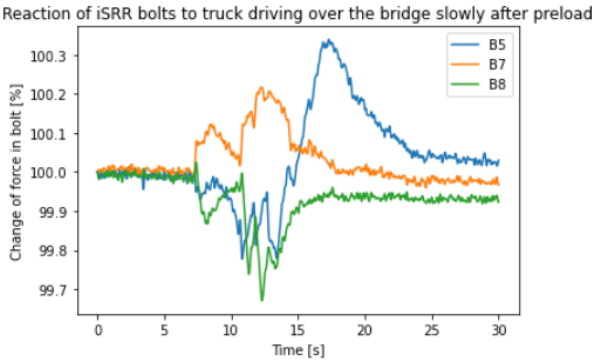

Figure 4.9: Force in iSRR bolts under truck loading after preload

4.1.4 Comparison of the connectors

To enable comparison between the bolt forces of the iSRR and Lindapter Hollo bolts, these have been presented in the same graphs in Figures 4.10 and 4.11. As in the previous Figures, the forces, both before and after reapplying the pre-tension, are expressed as percentages.

From these graphs, it can be concluded that the bolt forces resulting from the traffic load are very similar across both bolt types. Only one Lindapter Hollo bolt deviates in magnitude from the others. The remaining bolt responses are nearly equal in magnitude and represent relatively small forces compared to the applied pre-tension in the bolts.

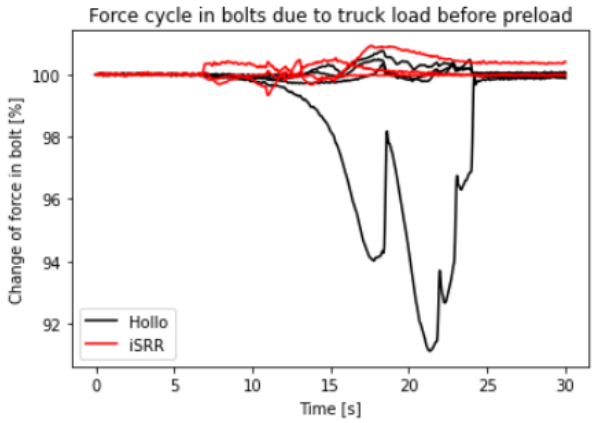

Figure 4.10: Force cycle due to truck load before preload

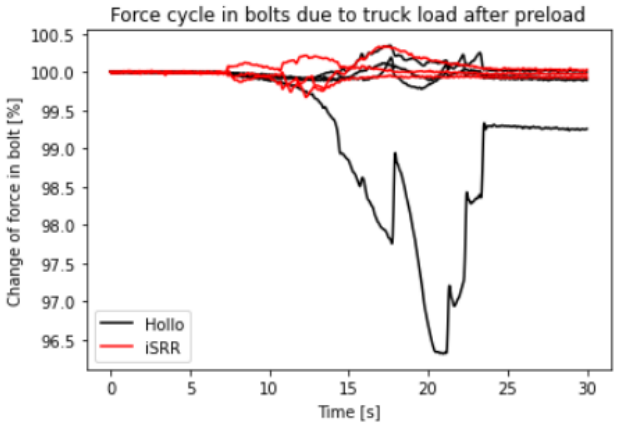

Figure 4.11: Force cycle due to truck load after preload

4.1.5 Hypothesis deviation bolt 2

The difference between bolt 2 and the other bolts could be caused due to inconsistent contact between the bridge deck, the crossbeam, and the clamping plate. This situation is illustrated in Figure 4.12. The dark grey clamping plate is shown on the left side, where it is connected to the bridge deck using the iSRR bolt connector, with a black rubber layer in between. A black arrow indicates the intended contact point between the clamping plate and the crossbeam, which is necessary to transfer forces through the bolts.

As visible in Figure 4.12, a polyethene (rubber) layer is present between the clamping plate and the crossbeam. Since there is also an interlayer between the clamping plate and the bridge deck, imperfections in these layers may result in uneven contact between the clamping plates and the crossbeam across different locations. A similar rubber interlayer exists between the bridge deck and the bridge crossbeams. Imperfections at this location can prevent consistent contact across the entire surface. As a result, forces caused by traffic and other loads may not be transferred uniformly, leading to variations in the bolt responses.

This explanation aligns with the relatively small bolt force responses observed under the traffic load from the truck.

In the case of Bolt 2, it appears that better contact is established, as its response to external loading is significantly greater than that of the other bolts. This suggests that, due to improved contact, forces are transferred to the crossbeam through this bolt even with a relatively small upward movement of the deck caused by traffic loading. Consequently, more representative forces are measured in this bolt compared to the others. This observation is consistent with the results from the bolt force measurements.

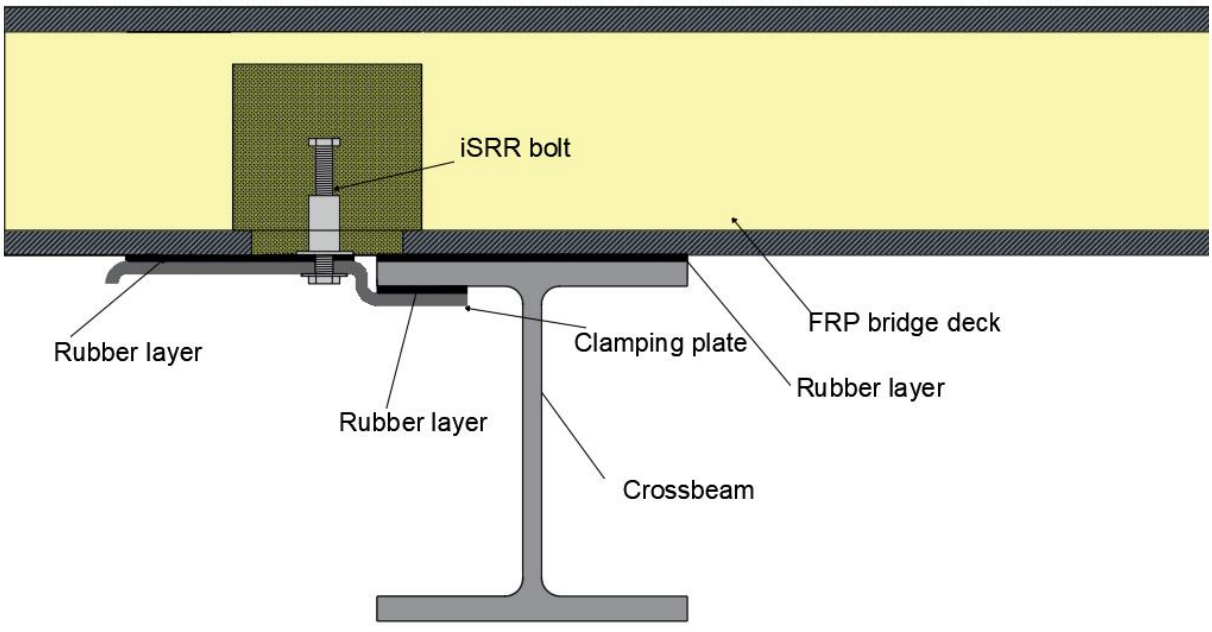

Figure 4.12: Rubber interlayers at iSRR connector

To test this hypothesis, the rubber interlayers between the clamping plates and crossbeams beneath the bridge were compared. Figures 4.13 and 4.14 show the clamping plates corresponding to bolts 2 and 6, respectively. The clamping plates at the other bolts have a situation comparable to that of bolt 6.

Figure 4.13 clearly shows that there is more space between the clamping plate and the bridge deck at bolt 2 than at bolt 6 in Figure 4.14. The rubber layer at bolt 2 appears slightly wavy and is less tightly compressed between the clamping plate and the bridge deck than at bolt 6. Additionally, the layer between the clamping plate and the crossbeam at bolt 2 is significantly less compressed than at bolt 6. For bolt 6, the clamping plate must be pressed more tightly against the bridge deck to achieve the required pre-tension in the bolt. This indicates that contact between the clamping plate and the crossbeam is less effective at bolt 6 than at bolt 2, which is consistent with the hypothesis.

It is therefore recommended to ensure uniform contact between all clamping plates and the crossbeam by installing additional shims and to also optimise contact between the bridge deck and the crossbeams. Subsequently, the measurement results before and after these adjustments should be compared.

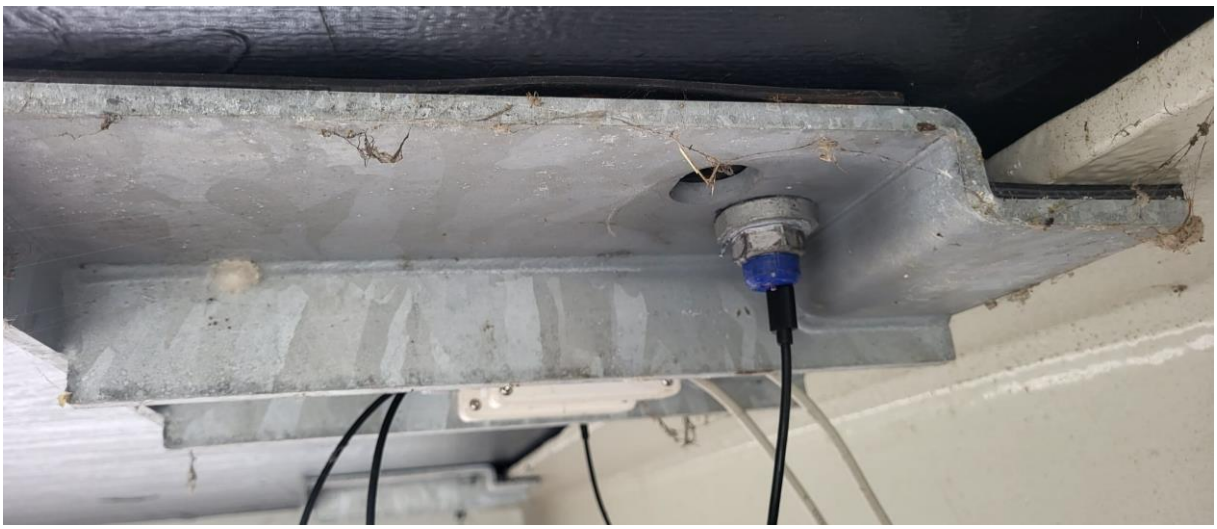

Figure 4.13: Clamping plate at bolt 2

Figure 4.14: Clamping plate at bolt 6

4.2 Opening of the bridge

The response of the bolts to the opening and closing of the bridge will be examined in this chapter. This is done both before and after reapplying the preload force to the bolts. The differences between before and after applying the preload force will be compared. After this, the reactions of both types of connectors will be compared, and conclusions will be drawn from there. At the time of the opening and closing of the bridge, there was a relatively low wind speed of less than 10 kilometres per hour. Because of this, it is assumed that the wind has no influence on the forces in the bolts.

4.2.1 Bolt forces before re-preloading

In Figure 4.15, the forces in the bolts are shown at the moment when the bridge opens and closes before reapplying the preload force to the bolts. The force is shown as a percentage of the force in the bolt before applying the load to make it easier to compare the forces in the bolts. From this Figure, it is evident that the opening and closing of the bridge has the most significant impact on the forces in Hollo bolts 2 and 3. The largest loads are in bolt 2, similar to the traffic loads. This appears to be a significant difference compared to the other bolts, but in absolute terms, it is only 4 per cent, which translates to a difference in force of around 0.5 kN. This is still a relatively small force compared to the preload force in the bolt.

Another observation is that bolt 3 reacts differently to the opening and closing of the bridge than the other bolts. While the force in the bolt decreases for all the other bolts, it slightly increases in bolt 3 during the opening of the bridge.

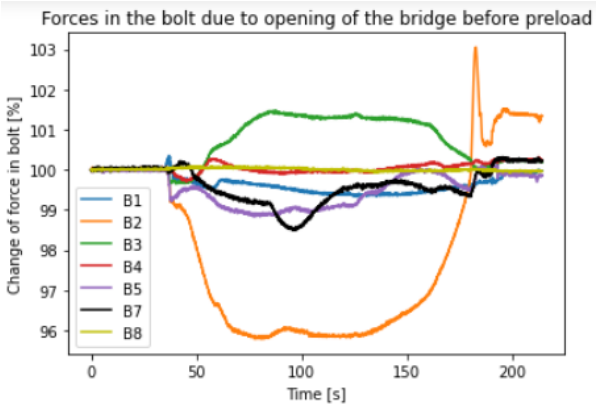

Figure 4.15: Forces in the bolts due to the opening of the bridge before preload

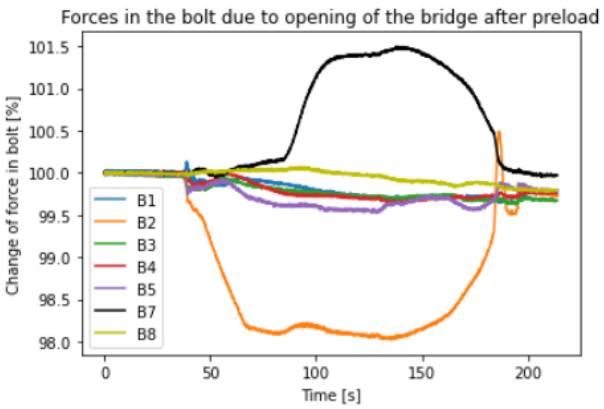

Figure 4.16: Forces in the bolts due to the opening of the bridge after preload

4.2.2 Bolt forces after re-preloading

The forces resulting from the opening and closing of the bridge after reapplying the preload force to the bolts are depicted in Figure 4.16. Once again, the forces in the bolts are shown as percentages for an easier comparison between the bolts. It is evident from this Figure that the percentage difference in bolt forces due to the bridge opening is approximately half as large as the differences observed

before reapplying the preload force to the bolts. Since the force in the bolts due to re-preloading is approximately twice as large as before, this means that the absolute difference in force remains roughly the same. Therefore, the higher preload force in the bolts does not affect the magnitude of the bolts 'response to the opening and closing of the bridge.

Another difference is that the force in the bolts does not return completely to 100% after the bridge is closed, while this was the case before reapplying the preload to the bolts. This is because the preload force decreases relatively quickly directly after application due to the rubber layer that is located between the bridge deck and the clamping plate. Additionally, it is noticeable that in bolt 7, the force in the bolt increases, unlike the other bolts. Furthermore, the response of this bolt is greater than that of all other bolts, except for bolt 2.

4.2.3 Comparison between the iSRR and Hollo connectors

In Figures 4.17 and 4.18, the forces in the bolts during the opening and closing of the bridge are shown as percentages of the force in the bolt before applying the load. The iSRR bolts are represented in red, while the Hollo bolts are depicted in black. Figure 4.17 illustrates that, before reapplying the preload force to the bolts, the response of the iSRR bolts is, on average, smaller than that of the Hollo bolts. After reapplying the preload force, one iSRR bolt and one Hollo bolt exhibit slightly larger responses than the others, this can be seen in Figure 4.18. However, all these responses, both before and after reapplying the preload force, do not exceed 4% of the present preload force. This translates to a difference of only 0.5 kN in the bolt. Hence, it can be concluded from these measurements that the differences in response between the two types of connectors to the loading from the opening and closing of the bridge are small. Additionally, it is evident that Hollo bolt 2, like in the case of the traffic load, exhibits the largest response among all bolts. This aligns with the previously mentioned hypothesis regarding the deviation of bolt 2.

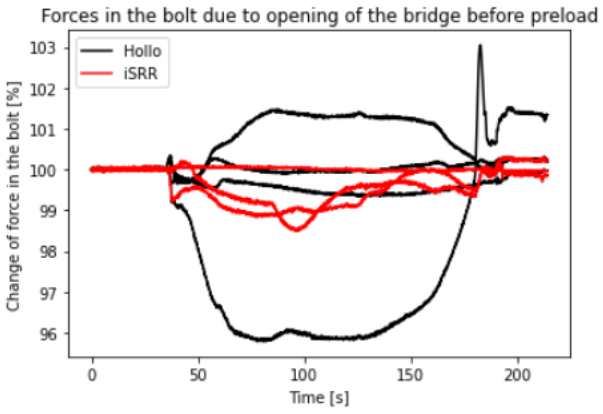

Figure 4.17: iSRR vs Hollo bolt forces for opening bridge before preload

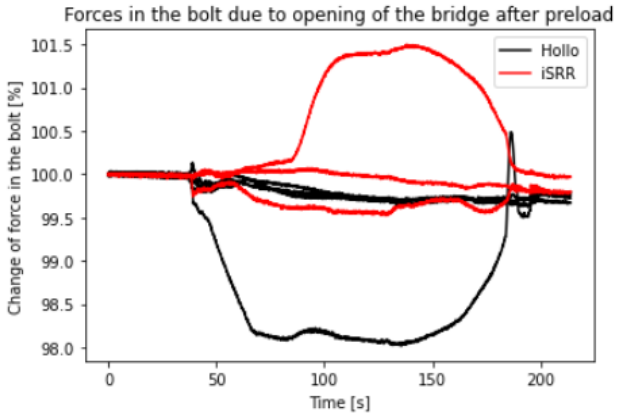

Figure 4.1818: iSRR vs Hollo bolt forces for opening bridge after preload

4.3 Influence of the temperature

Before evaluating the loss of preload in both types of connectors, the influence of temperature on the bolt forces is first examined. This step is essential to determine whether the temperature has a significant impact on the measured bolt forces and should therefore be considered in the assessment of preload loss.

To investigate this, the bolt forces and corresponding temperatures over a 15-day period immediately following the initial preloading were plotted together. In these Figures, bolt force is shown on the left vertical axis, while temperature is represented on the right. This analysis was performed for the Lindapter Hollo bolts (Figure 4.19) and the iSRR bolts (Figure 4.20).

From both Figures, it is clearly visible that temperature has a substantial influence on bolt force, with variations of several kilonewtons observed over just a few days. The only exception is bolt 2, where the changes in bolt force, due to the temperature fluctuations, are considerably smaller compared to the other bolts. For the other bolts, a temperature change of 15 °C leads to a change of force in the bolt of around 2.5 kN. Therefore, it can be concluded that the effects of temperature must be accounted for when analysing preload losses in the bolts.

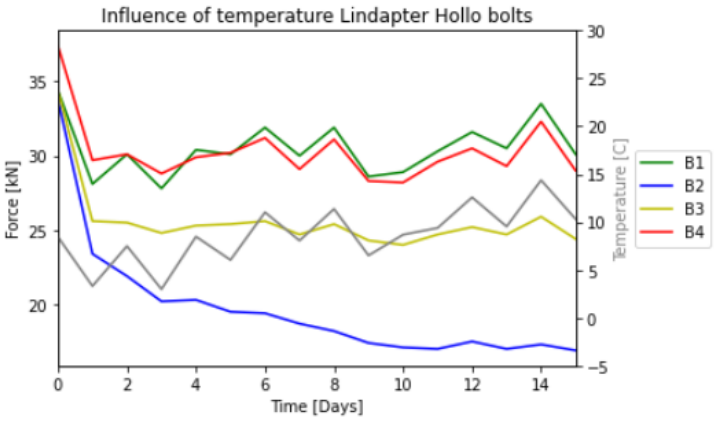

Figure 4.1919: Impact of temperature on Lindapter Hollo bolts

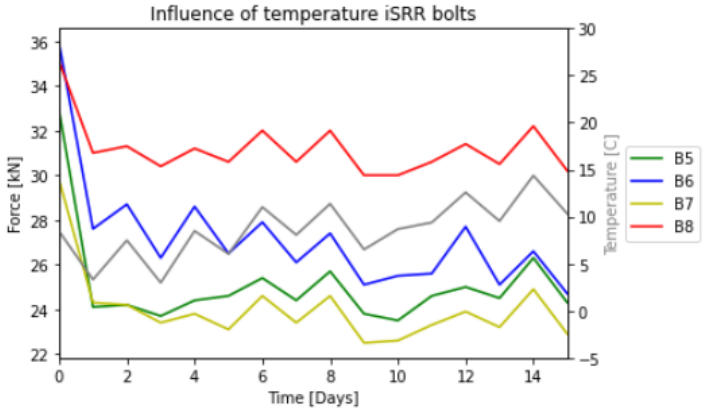

Figure 4.2020: Impact of temperature on iSRR bolts

4.4 Loss of preload

In this chapter, the loss of preload in the bolts over time will be examined. These losses will be compared for the different types of connectors. The force in the bolts has been tracked every day for an extended period to measure the loss of preload of the bolts. This period, that is nearly 250 days, provides a clear picture of the prestress loss for both types of connectors. Due to technical issues, a part of the data from this period is missing. But there is sufficient data to compare the loss of preload effectively and draw conclusions.

A preload force of approximately 35 kN was applied to all bolts at the start of the period of measuring. Due to the presence of a rubber layer between the clamping plate and the bridge deck, it was not possible to have exactly the same preload force for all of the bolts. This rubber layer is placed in a similar manner for both types of connectors. This rubber layer is illustrated in Figure 4.21 and 4.22 for both connector types. The rubber layer has been indicated in black and is marked with a red arrow. Because the initial preload of each bolt is not exactly the same, both the absolute and percentage loss of preload force in the bolts will be examined to facilitate better comparisons of the losses.

The preload losses of the Hollo bolts will first be examined in this chapter. After this, the preload losses in the iSRR bolts will be looked at. Finally, these losses will be compared for both types of connectors.

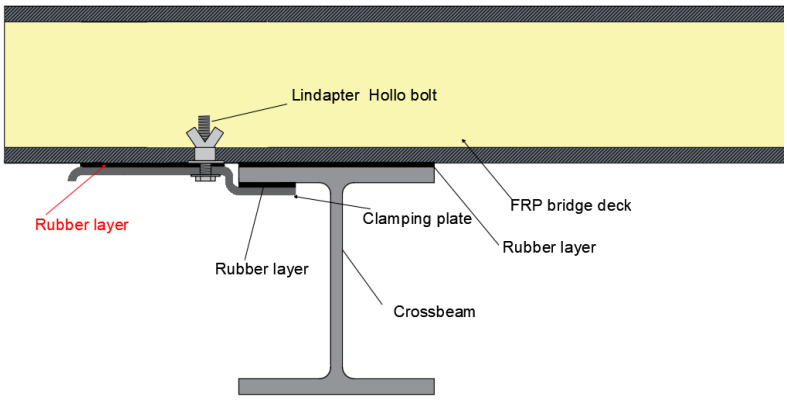

Figure 21.21: Lindapter Hollo bolt connector

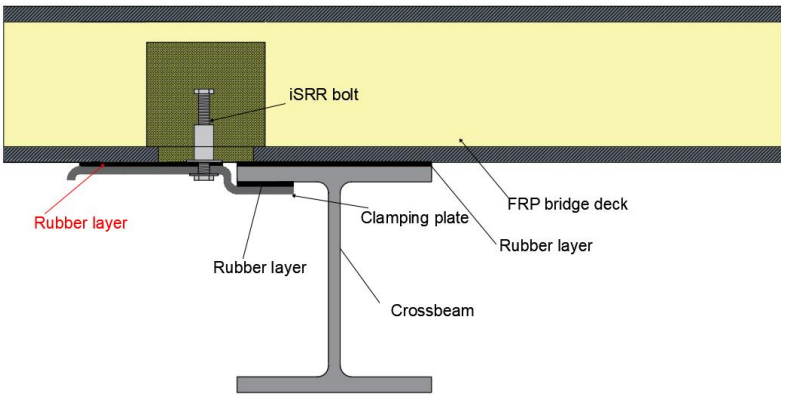

Figure 22: iSRR connector

4.4.1 Lindapter Hollo bolts

The preload force in the Hollo bolts for a period of nearly 250 days is displayed in Figure 4.23. In this Figure, the force in the bolt is shown on the left vertical axis in kN. The time in days is displayed on the horizontal axis. Additionally, a second vertical axis on the right has been used to indicate the temperature on each day. This is included because there is a clear influence of the temperature on the forces in the bolts. The temperature on each day is represented by the grey line in the Figure. In the left part of the Figure, it is visible that the forces in bolts 1, 3 and 4 have a very similar pattern to the temperature line, after the initial loss of preload shortly after applying the preload force. Higher temperatures lead to higher forces in the bolts and vice versa. The influence of temperature is also somewhat visible in bolt 2, but the correspondence with the temperature line and the magnitude of the response is less than with the other bolts.

After almost 250 days, the preload force for the Hollo bolts is close to each other, ranging between 12 and 16 kN for all bolts. This is between 40 and 50 per cent of the initial preload force applied to the bolts. The temperature on the last day of measurement is much lower than when the prestress force was applied, so these percentages are lower than they would be if the temperature was the same. It is visible in Figure 4.23 that the preload in the bolts decreases rapidly in the first few weeks after applying the preload force. This is better visible in Figure 4.24, where the preload in the Hollo bolts is shown for the first 16 days. In this relatively short period, it is possible to eliminate the influence of the temperature on the force in the bolts. This is because there can be chosen a moment each day where the temperature is the same. This makes the loss of preload better visible. However, small peaks are still visible in the graph on day 4,6 and 11. This is likely due to the influence of the sun. This causes the bridge deck and thus the bolts to warm up, potentially making them slightly warmer than the measured outdoor temperature under the bridge.

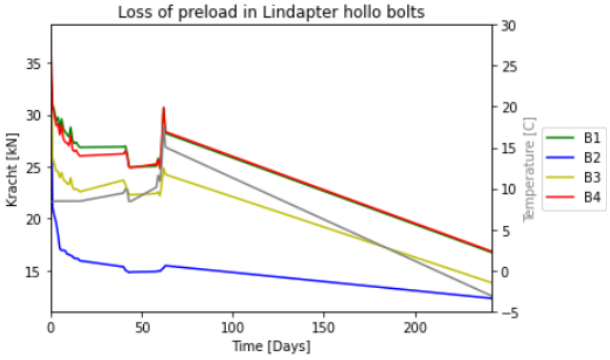

Figure 4.23: Loss of preload Lindapter Hollo bolts

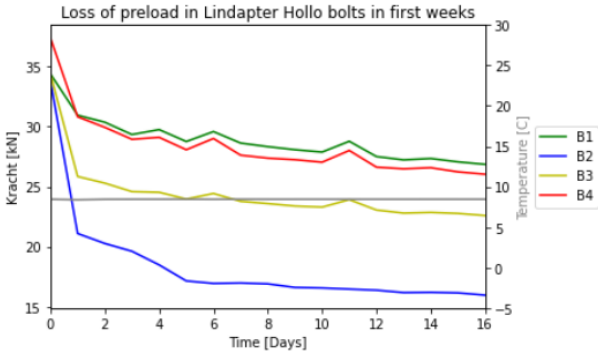

Figure 23.24: Loss of preload Lindapter Hollo bolt in first weeks

Looking at the graphs, it is clear that for all bolts the preload decreases the most in the first 4 days after applying the preload force. After these first four days, the force in the bolts decreases less rapidly. The cause for the greater loss of preload force in the first few days is the rubber layer present between the clamping plate and the bridge deck. Relaxation of the rubber interlayer seems to cause the tensile preload force in the bolts to decrease relatively quickly at the beginning. This decrease in force is not exactly the same for all bolts. This could be caused due to imperfections in the rubber interlayer and small differences in the orientation of the clamping plate. After the first week, the tensile force in the Hollo bolts decreases at a slower rate. This rate is similar for all Hollo bolts. After 75 days, the preload in bolts one, three and four decreases at almost exactly the same rate. In bolt two, the preload decreases less rapidly than the others.

4.4.2 iSRR bolts

The preload force in the iSRR bolts over the period of nearly 250 days is depicted in Figures 4.25 and 4.26. Both Figures utilise two vertical axis I the same way as the Figures of the Hollo bolts in the previous section. For bolt 6,there is no final value of the force in the bolt known at the end of the period. This is why bolt 6 is absent in Figure 4.25 but present in Figure 4.26.

In the first 60 days it can be observed that the temperature has a similar impact on the iSRR bolts as it has on the Hollo bolts. A higher temperature leads to higher forces in the bolts and the forces are lower at lower temperatures. At the end of the period of almost 250 days, the force in bolts 5 and 7 is close to each other, both having around 15 kN remaining of the initial preload force. This equates to approximately 50% of the applied preload force. Bolt 8 performs significantly better, retaining a preload force of almost 25 kN at the end of the period. This is nearly 70% of the initial applied preload force. The main cause for this difference between the bolts occurs after 70 days. After the first months, the preload force in bolts 5 and 7 decreases at a similar pace. But it decreases at a much lower rate in bolt 8.

In Figure 4.26, where the temperature is kept constant, it is visible that the preload force in the bolts decreases the most on the first day after applying the preload force. This is likely due to the presence of the rubber interlayer between the clamping plate and the bridge deck. After this first day, the force decreases for all iSRR bolts at a comparably slower pace. Small peaks are visible in the graphs at the same days as the Hollo bolts. This will likely be due to the influence of the sun. Even in the first 16 days, it is evident that bolt 8 is performing better than the other iSRR bolts, experiencing less preload loss. However, the bolt force in this Figure decreases at a similar pace after the first day, which is not the case after a longer period.

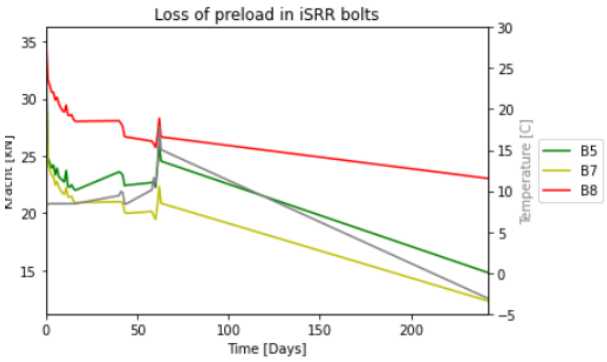

Figure 24: Loss of preload of iSRR bolts

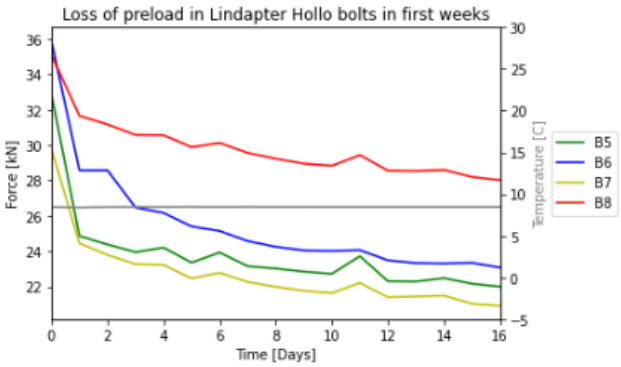

Figure 25: Loss of preload of iSRR bolts in the first weeks

4.4.3 Comparison for both types of connectors

To compare the preload force in the iSRR bolts and Hollo bolts, the forces in both bolts are displayed in Figures 4.27 and 4.28. In Figure 4.27, the absolute forces over the period are represented in black and red, while the temperature is shown in blue. In Figure 4.28, the forces are displayed as percentages relative to the initial preload force in the bolt, making it easier to compare the loss of preload force for the two types of connectors.

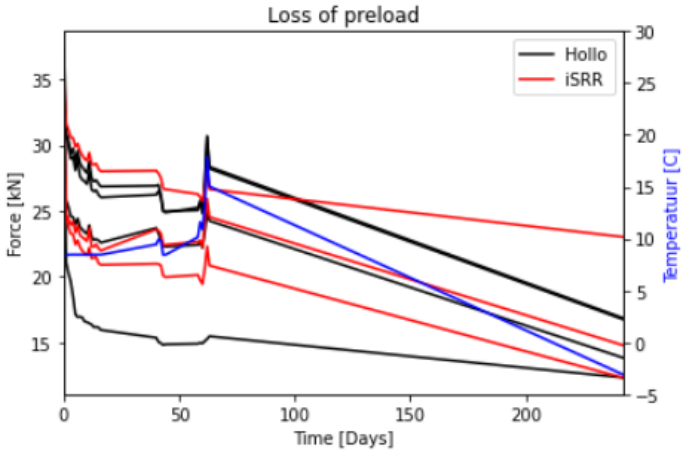

Figure 26: Loss of preload of the bolts

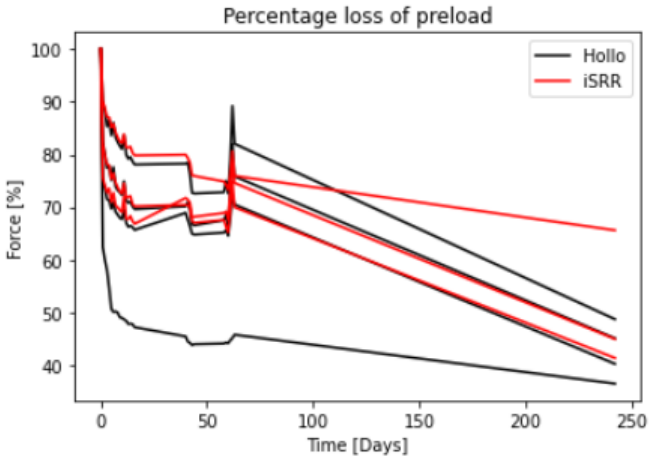

Figure 27: Percentage loss of preload of the bolts

In both Figures is visible that the force in the bolts is relatively close to each other throughout the period. Both types of connectors lose a significant amount of preload shortly after applying the preload force, with approximately 77.5% of the initial preload force remaining in the bolt after the first day. With exception of one iSRR bolt, the final preload force of all bolts is between 40% and 50% of the initial preload force in the bolt. On average, the iSRR bolts retain more preload force after this period, with 50.6%, compared to the Hollo bolts, which have an average of 42.7% of the preload force remaining in the bolt. This is mainly due to the behaviour of bolt 8, which performs better than all of the other bolts. Bolt 8 loses much less preload and retains almost 70% of the preload force after nearly 250 days. Apart from this bolt, there are no clear differences in performance between the two types of connectors. The main cause for this could be the presence of the rubber interlayer between the clamping plate and the bridge deck. This seems to be the main reason for the preload loss in both connector types. To better assess the potential differences in behaviour of the connectors, an experiment is needed where the bolts are preloaded without the presence of a rubber interlayer at the bolts. An example of this is to have the rubber interlayer only present at the end of the clamping plate. This way, the positive effects of the rubber like the coping with imperfections will still be utilised while the impact on the preload force in the bolts over time, caused by this interlayer, will be eliminated. Then, the effect of the SRR injection, which should result in a slip-resistant connector, on the retention of preload force in the bolt connector could become visible.

4.5 Long-term effects

In addition to short-term effects, long-term effects are also being considered. To assess these, monitoring will be conducted at the Ulsderbrug over a period of 1 to 4 years. This approach will provide a comprehensive understanding of the volume of traffic crossing the bridge throughout different times of the year, and the corresponding impact on both types of connectors over time. At present, 211 days of data are available.

Before analysing this dataset, the required steps for data analysis are first explained using a small sample to illustrate how the data is acquired and how load cycles are counted. For this purpose, a one-week period is used, covering Wednesday, 20 March 2024 to Tuesday, 26 March 2024. The analysis focuses on the force measured in Bolt 2, as this bolt exhibits the largest reaction forces. As a result, traffic events are clearly visible in the data, and different vehicle types can be distinguished with relative ease.

To determine the impact of load cycles on the fatigue behaviour of both connector types, the rainflow counting method is applied. Figures 4.29 and 4.30 illustrate how the extreme values are processed and which data remains from the force measurements in the bolt. Figure 33 displays the force in Bolt 2 during several controlled passes of a passenger car driving back and forth over the bridge. The force is recorded at 0.02-second intervals. Figure 4.30 shows the identified peaks and troughs over the same time period. Lines are drawn between these points to demonstrate the correspondence of these extreme values with those in Figure 4.29.

In both Figures, it is evident that each axle of the car generates a distinct peak during passage. Additionally, all peaks and troughs present in Figure 4.29 are also found at corresponding positions in Figure 4.30. In this manner, all load cycles are efficiently captured and included in the analysis.

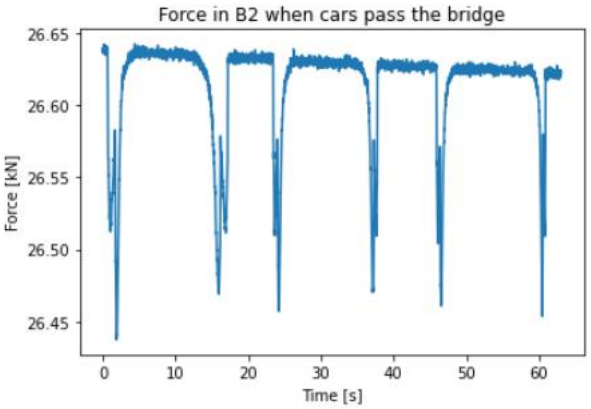

Figure 28: Force in bolt 2 when loaded by traffic

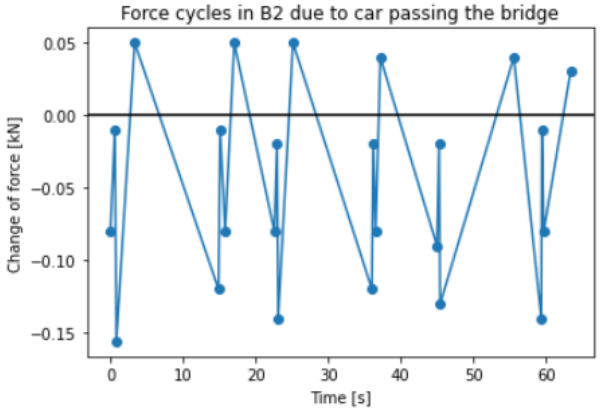

Figure 4.30: Peak values of force cycle due to traffic loading in bolt 2

Figure 4.31 presents the load cycles in bolt 2 over the entire monitoring period of 220 days. These load cycles range from -2.0 kN to 1.0 kN. The Figure shows three short gaps in the data, totalling approximately nine days, during which the monitoring equipment did not function properly. Consequently, these days were excluded from the analysis, which was conducted using the remaining 211 days of data.

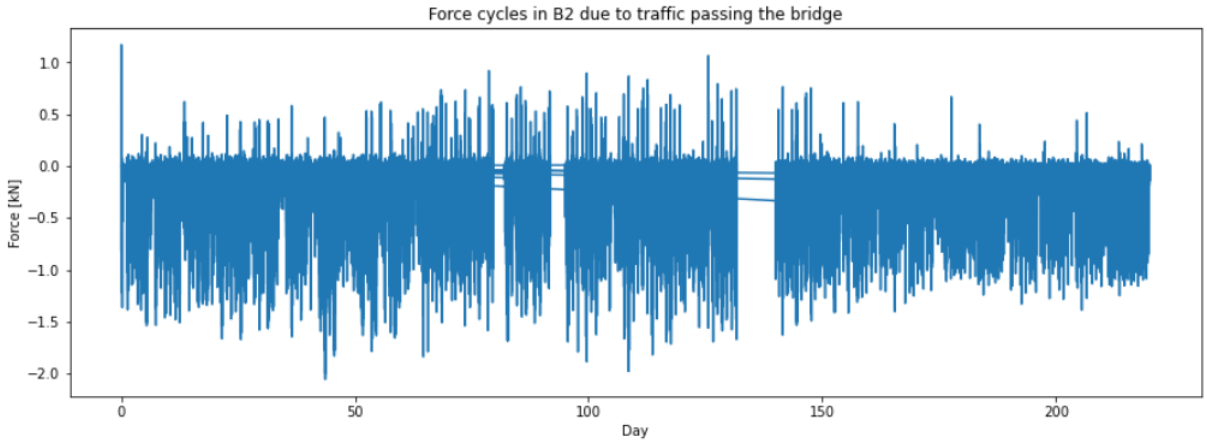

Figure 4.3129: Force cycles in Lindapter Hollo bolt 2 for a period of 211 days

Figures 4.32 and 4.33 present bar charts of the load cycles. To accurately assess the volume of traffic crossing the bridge, the cycles are categorized by magnitude. In both Figures, a bin size of 0.1 kN is used. It is clearly evident that the majority of load cycles exhibit a force variation of less than 0.25 kN, which primarily corresponds to passenger vehicles.

The load cycles exceeding 0.25 kN are shown again in Figure 4.33 to clearly illustrate their frequency. These larger cycles are associated with heavier vehicles crossing the bridge, such as trucks and tractors. These bar charts provide an effective means of monitoring the traffic volume over the bridge.

Over the 211-day period, 322,356 load cycles with a force difference smaller than 0.25 kN were recorded, corresponding to more than 160,000 passenger vehicles. Additionally, 44,294 load cycles exceeding 0.25 kN were identified during the same period. However, translating this number into a precise count of heavy vehicles is more complex due to variations in axle configurations.

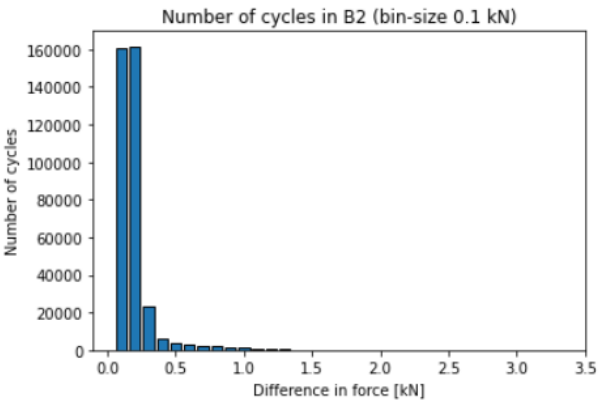

Figure 30.32: Force cycles in bolt 2 distributed by size

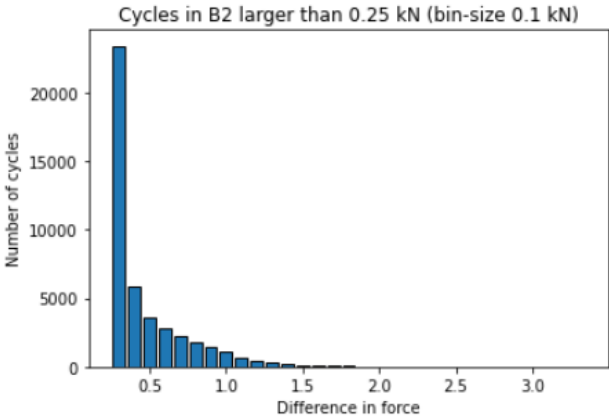

Figure 4.33: Force cycles larger than 0.25 kN

To assess the impact of traffic on the fatigue behaviour of the bolts, the Eurocode (1993-1-9+C2, 2012) is applied. This standard allows for the evaluation of whether the stress amplitude in the bolts, in combination with the number of load cycles, contributes to fatigue and thus affects the service life of the bolts.

Bolts subjected to axial (normal) stress fall under detail category 50. The corresponding fatigue strength curve is shown in Figure 4.34. The fatigue limit for this category is 37.25 N/mm². The highest load cycle observed in the bolts was 1.95 kN, corresponding to a stress cycle of 9.70 N/mm². Extrapolating from the controlled load, this would be caused by a vehicle of approximately 43 tons. Assuming that the number of axles and load distribution of this load are similar to that of the controlled load. The stress cycle of 9.70 N/mm² lies well below the fatigue limit of 37.25 N/mm², indicating that the stress cycles in the bolts caused by traffic loads on the bridge do not affect the bolts' service life.

To see whether these forces impact other parts of the connector, other than the bolt, we can look at other research done for this connector. J. Köhlenberg investigated the ultimate resistance of the iSRR connector due to wheel loading using cyclic tests. From this research can be concluded that the connector does not experience fatigue damage for a load cycle of 9-90 kN after 2.1 million cycles (J. Köhlenberg, 2023). This load cycle is significantly higher than the largest load cycle monitored at the bridge. Which means that the service life of the iSRR connector will not be affected by the traffic loads.

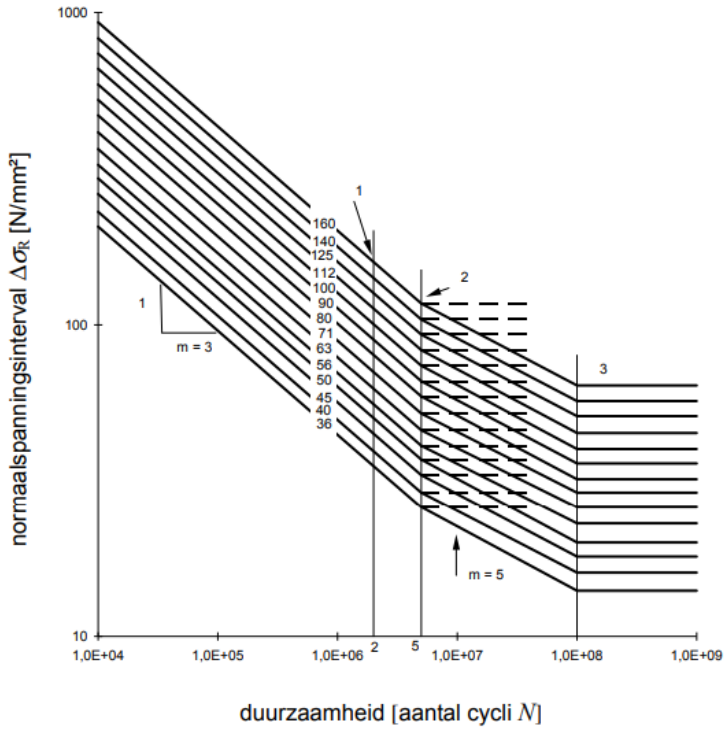

Figure 4.3431: Fatigue strength curves for normal stress intervals (1993-1-9+C2, 2012)

5. Finite Element Model

To investigate the predictability of the tensile forces in the connectors, a finite element method model is used. The finite element model has been designed using SOFiPLUS and has been analysed using Sofistik (Sofistik, 2023). The bolt forces predicted by the model will be compared to the measured forces in the bolts of the bridge. The model used for this will be discussed in this chapter. First a description of the model is given including boundary conditions, material properties, assumptions and what limitations follow from this. Secondly will be explained what type of analysis has been used. After this will the verification of the model be discussed. Finally the predictability of the forces in the connector can be concluded.

5.1 Model definition

The composite bridge deck is modelled using shell elements and is positioned on top of the crossbeams of the bridge. This is illustrated in Figure 5.1. This Figure also shows the orientation of the axes of the model. The x-axis (red arrow) is directed in longitudinal direction, the y-axis (green arrow) is directed in transversal direction and the z-axis (blue arrow) is directed in vertical direction. The crossbeams of the bridge are connected to the longitudinal girders, which are supported at both ends.

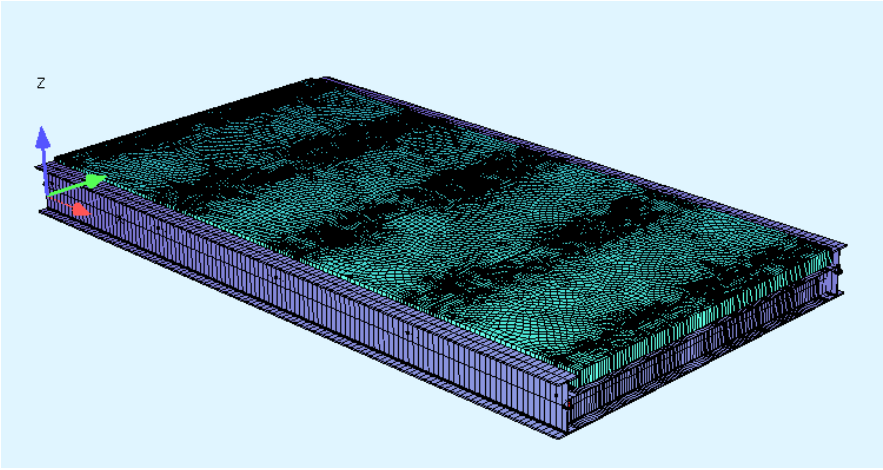

Figure 32.1: Axis orientation of the model

The FRP bridge deck, designed by FiberCore, can structurally be seen as a sandwich construction composed of three layers. The two facings, at the top and at the bottom of the deck, are made of glass fibre-reinforced polyester (GFRP). In between these facings is a shear-rigid, fibre-reinforced core. This core consists of web plates that connects the upper and lower layer of the bridge. These web plates transfer the shear forces to the supports. The rest of the middle layer consists out of foam, which is mainly used for manufacturing purposes. The structural properties will not be considered in the calculations because the long-term structural behaviour of the foam core can't be reliably guaranteed.

The bridge deck has been modelled in a similar way as it was by FiberCore when designing the deck. The deck is built up out of three layers. The top and bottom layer have the same thickness, material layup and properties. The middle layer of the deck makes up the largest part of the deck and has a considerable lower stiffness than the top and bottom layer. The thickness and stiffness of each layer can be found in table 5.1.

Table 5.1: Bridge deck layers

Layer	**Thickness [mm]**	**Stiffness [GPa]**
Top	21.0	28.0
Middle	246.0	0.45
Bottom	21.0	28.0

A bottom view of the model of the bridge is displayed in Figure 5.2. This Figure shows the locations of the four supports of the bridge. These supports are located at the ends of the longitudinal girders and are displayed in red. It also gives insight into the location of the bolted connectors, which are the light green coloured springs. The longitudinal girders and the crossbeams differ in dimensions. The longitudinal girders are a HEA profile with a height of 911 mm and a width of 418.5 mm. The crossbeams are also a HEA profile but have a height of 590 mm and a width of 450 mm. These dimensions are for both beams constant of the length of the beam. Figure 5.3 shows the dimensions of the beams of the bridge and the distances between the middle points of the clamping plates. The clamping plate is showed in more detail in Figure 5.6.

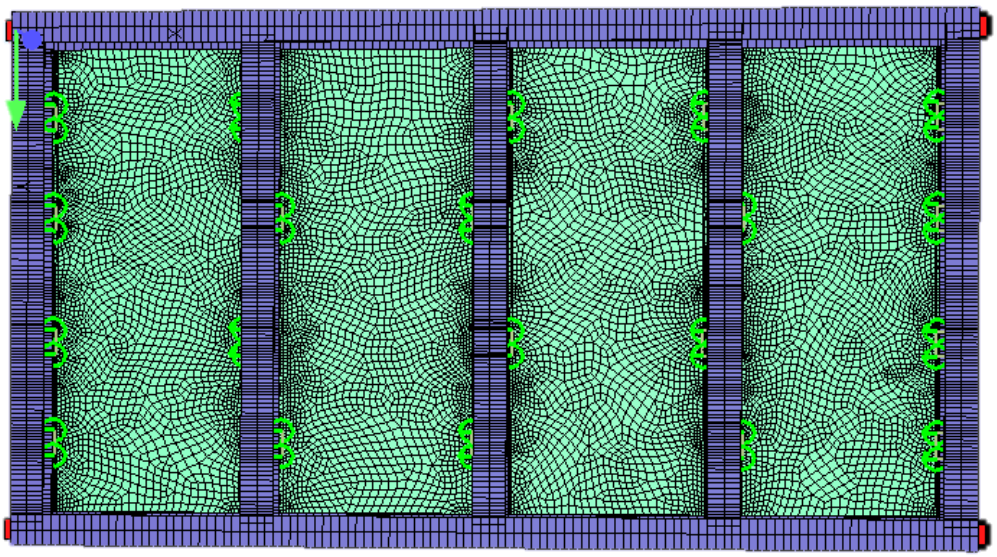

Figure 33: Bottom view of the model

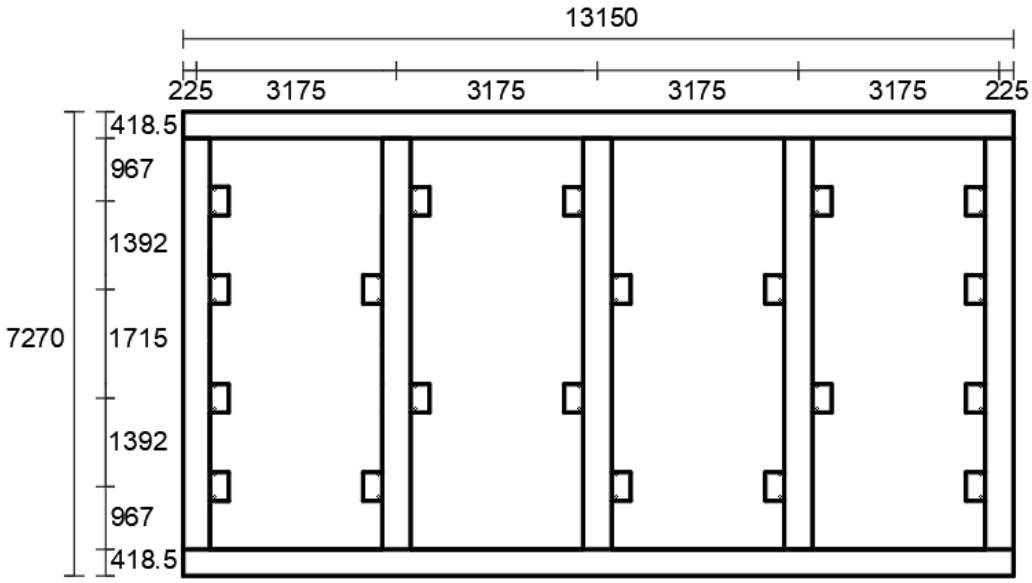

Figure 34: Dimensions of the bridge [mm]

In the model, both types of bolted connectors are modelled as springs that can only transfer tensile forces. This reflects the actual behaviour of the bolts of the bridge, that can only transfer tensile force due to the way the connection is designed. Figure 5.4 illustrates the way the bolts are modelled. The bolts are represented in this Figure by the red springs. These springs are connected to the clamping plate at the bottom of the springs. The red circles at the top of the springs is the point where the springs connects with the FRP bridge deck. All the bolts have been preloaded with a force of 35 kN in the model, this is the same preloading force that has been used at the bridge. The bolts are connected to the crossbeams via clamping plates to facilitate further force transmission to the crossbeams of the bridge. These clamping plates have a thickness of 10 mm. The other dimensions of the clamping plate are illustrated in Figure 5.6.

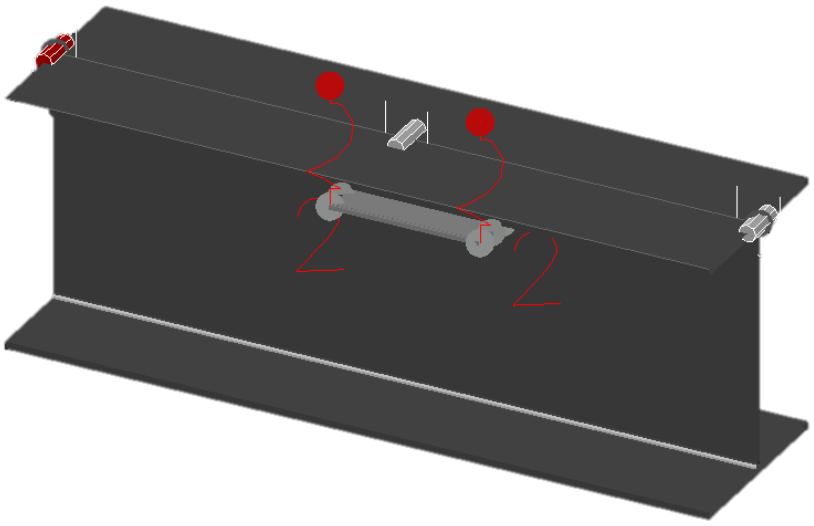

Figure 5.4: Bolts modelled as springs

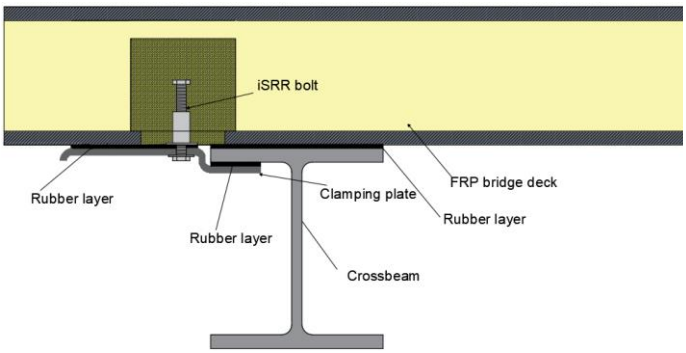

Figure 5.5: Design detail of the iSRR connection

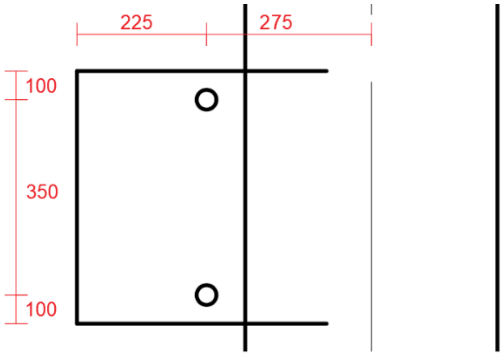

Figure 5.6: Bottom view of the clamping plate with dimensions (in mm)

Figure 5.5 illustrates how the clamping plates connects an iSRR bolt with the crossbeam of the bridge. The clamping plate connects the Lindapter bolts in exactly the same way with the crossbeams of the bridge. Figure 5.5 also shows the three different rubber layers that are present at the bolted connector. These three rubber layers are present in exactly the same way for both connector types. The first rubber layer is located in between the bridge deck and the crossbeam of the bridge. The second layer is in between the clamping plate and the crossbeam. And the final layer is in between the bridge deck and the clamping plate. All three of these rubber layers have an impact on the force in the bolts and therefore have to be implemented in the model. The three rubber layers have all been modelled the same way using springs that can only transfer compressive forces. This reflects the actual nonlinear behaviour of the rubber, that can transfer compressive forces but is not able to transfer tensile forces. A work law has been used for the rubber layers to implement this in the model. Using this work law, the springs can be made nonlinear so they are not able to transfer tensile forces. The stiffness of the work law of the rubber layer in between the bridge deck and the crossbeam has a significant impact on the force cycle in the bolt when subjected to the truck load. Therefore has this stiffness has been varied to get an accurate force prediction for all of the bolts. Seven of the eight bolts have the same work law with a stiffness of -1 mm per 1000 kN, while another work law has been used for bolt 2 with a stiffness of -140 mm per 1000 kN. Both work law can be seen in the Figures 5.7 and 5.8 respectively for bolt 2 and for all the other bolts. The impact of the stiffness of the rubber interlayer will more extensively be discussed later in this chapter.

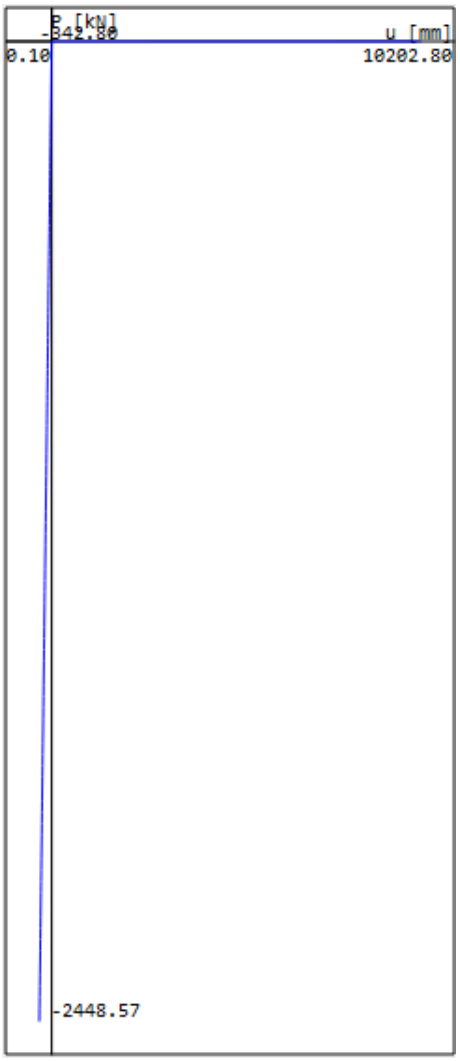

Figure 5.7: Work law of the rubber used for bolt 2

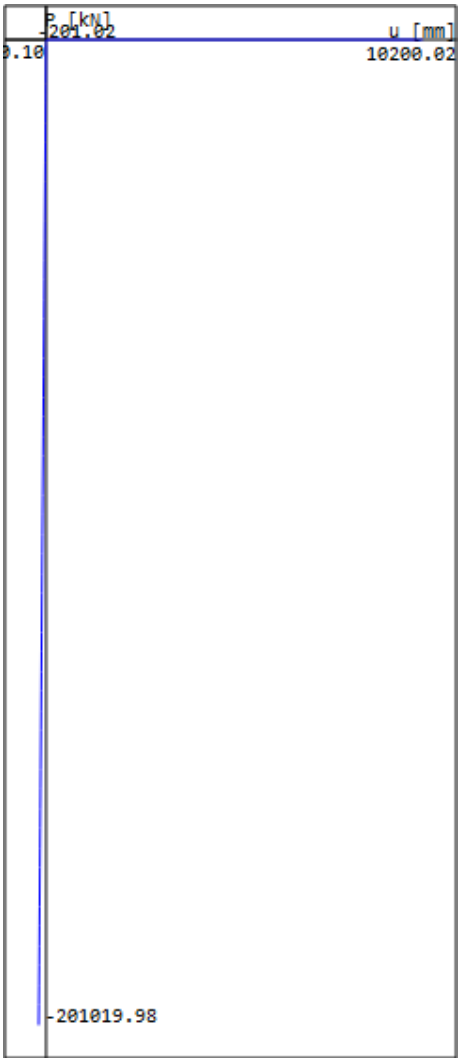

Figure 5.8: Work law of the rubber used for the other bolts

5.2 Analysis

Because of the nonlinear characteristics of the bolts and the rubber interlayers in the model of the bridge, a nonlinear analysis will be used in Sofistik to calculate the forces in the bolt. This analysis uses a nonlinear approach for all springs in the model, while the beam elements will be analysed with linear stress-strain characteristics. The code used for the nonlinear analysis can be found in Figure 5.9. This code will be explained briefly.

SYST PROB NONL is used to activate a material non-linear analysis with 1000 iterations (iter 1000). A direct parallel sparse solver (CTRL solv 4) has been used. The advantage of the direct solvers is especially given in case of multiple right hand sides, as the effort for solving them is very small compared to the triangulization of the equation system. Thus they are the first choice for any dynamic analysis or in case of many load cases. This solver PARDISO uses processor optimised high performance libraries from the Intel Math Kernel Library MKL. It usually provides the least computing times. It does not require an a priori optimisation of the equation numbers during system generation.

Beam, cable and truss elements are analysed with a linear material behaviour (NSTR s0). Spring elements are analysed with a non-linear spring work law if defined. The non- linear spring effects GAP, CRAC, YIEL and MUE are taken into account in a nonlinear analysis.

This code is only for load case one (see line 8) and will be repeated for all analyses done on the bridge.

```
1  prog ase urs:31.1
2  head
3  ctrl solv 4
4  ctrl iter 3 V2 10
5  syst prob nonl   iter 1000
6  NSTR s0
7  $grp 5 prex 35
8  lc 1 titl "LC1"
9
10 end
```

Figure 5.9: Analysis used in Sofistik

5.3 Limitations of the model

The finite element model approximates the characteristics of the actual bridge but, as every model, comes with its limitations. This is because not everything can be modelled exactly the same as the actual bridge and assumptions are made in the model definition.

The first limitation of the model is for the crossbeams of the bridge. The top of the crossbeams has been modelled flat over the length of the crossbeam while this is under a small angle at the bridge. At the actual bridge is the crossbeam 55 mm higher at midpoint of the beam compared to the height at both ends of the crossbeam. This slight angle has not been implemented in the model because a flat top of the crossbeam is easier to model and this angle has a minor influence on the forces in the bolts. Therefore this will not have a large impact on the results that follow from this model.

This first limitation also impacts the orientation of the bridge deck that is on top of the crossbeams. Because the bridge deck is located directly on top of the crossbeam, the bottom of the deck is also placed under the slight angle at the bridge. But because the top of the crossbeams has been modelled horizontally, the bottom of the deck has also been modelled horizontally to match the orientation.

The second limitation of the model is that the imperfections at the bridge are not taken into account. This is mainly relevant for the rubber interlayers at the bridge. The differences between these rubber layers in stiffness, placement and thickness have a significant impact on the forces in the bolt when loaded by passing vehicles, but are not possible to model exactly in the same way as they occur in real life.

Finally, the third limitation of the model is that it only takes short-term effects into account. This model is not able to predict the forces in the bolts after a longer period, where factors like creep, relaxation and fatigue come into play. This is especially relevant for the rubber layers, since the complicated behaviour of rubber is time-dependant and the reaction of rubber to loading varies.

5.4 Verification

The measurements that have been done at the bridge make it possible to accurately verify the precision of the forces in the bolts predicted by the finite element model. Because a truck with known dimensions and mass has driven over the bridge in a controlled manner, this load can replicated exactly in the same way in the model. The load used in the model consists out of eight wheel loads, displayed in Figure 5.10 as red squares. Each wheel load is 500 mm by 500 mm and distributes a load of 510.4 kN over this area. To simulate the truck driving on top of the bridge, the analysis consists of 43 load cases. In each load case the truck load is moved 500 mm in longitudinal direction over the bridge. The direction of the movement and the location of the truck load at the first load case are illustrated in Figure 5.10. This Figure also shows which bolts have been monitored at the bridge and therefore will be compared with the model to conclude the predictability of the bolt forces.

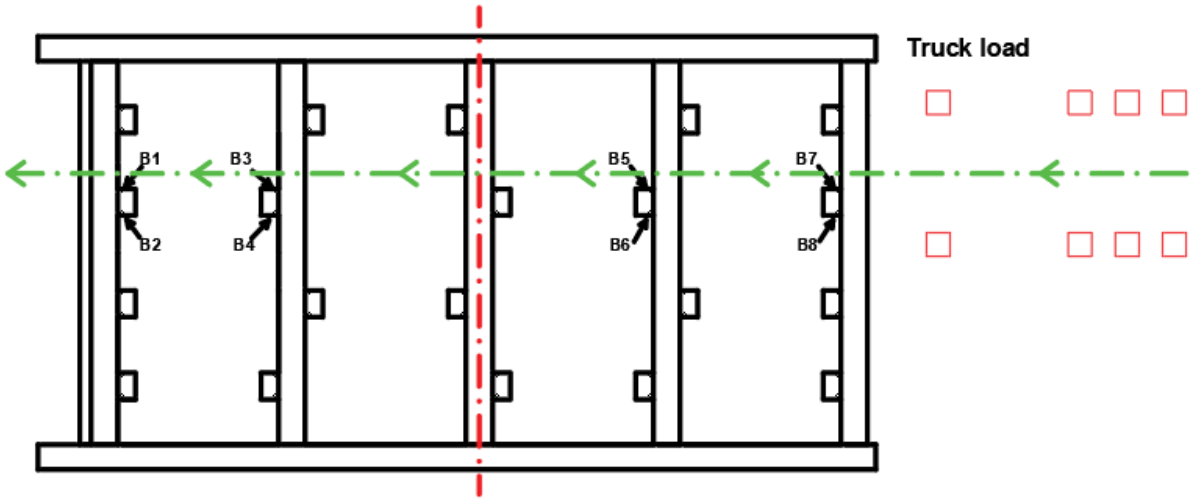

Figure 35: Truck load used in the model

The force cycles resulting from the nonlinear analysis of the model under truck loading are presented in Figures 5.11 and 5.12 for bolts 2 and 8, respectively. These specific bolts have been selected to represent the full range of monitored bolts. Bolt 2 was chosen due to its distinct response to the truck load compared to the other bolts. The other bolts are represented by bolt 8, because they react in a similar way when being loaded as bolt 8. Thus, analysing these two bolts provides a sufficient basis for verifying the accuracy of the model. In addition to the force cycles that follow from the nonlinear analysis, the actual measured forces for these two bolts are also displayed in these Figures. This allows a direct comparison with the predictions done by the model.

For both bolts, the model demonstrates a strong capability in predicting the force cycles. This is particularly evident for Lindapter bolt 2, shown in Figure 5.11, where the predicted force cycles from the SOFiSTiK model closely match the measured data. The comparison for iSRR bolt 8 is shown in Figure 5.12. While the model accurately represents the general magnitude of the force cycle, the agreement is not as strong as for bolt 2. A possible explanation for this discrepancy is that the forces in these bolts are significantly lower than those in bolt 2.

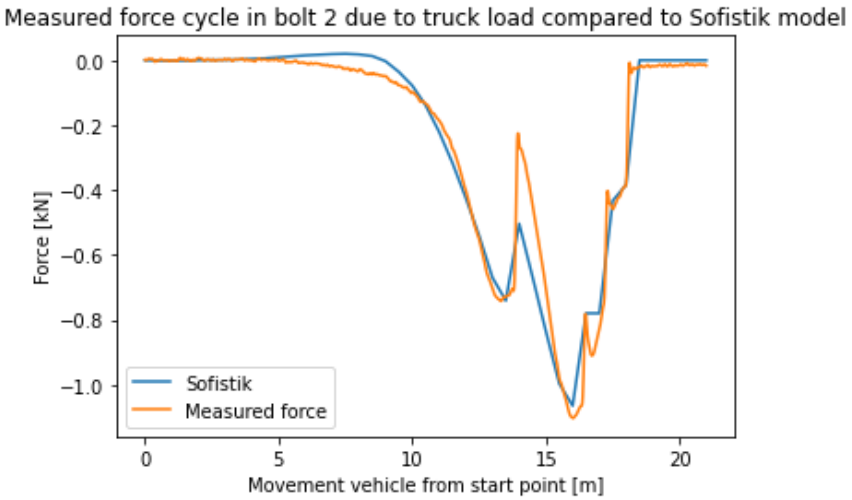

Figure 5.11: Verification of the model for bolt 2

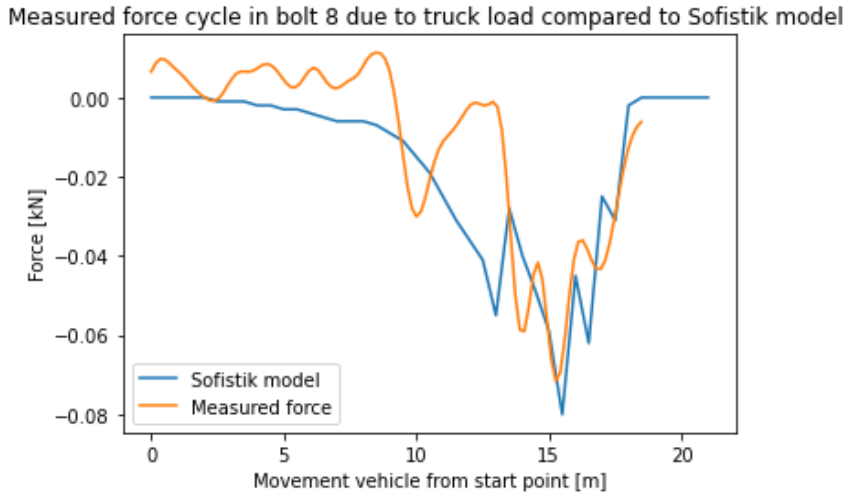

Figure 5.12: Verification of the model for bolt 8

The predicted bolt forces closely correspond to the measured forces obtained from on-site monitoring. In addition to this comparison, it is important to verify whether the model also produces realistic deformations under the applied loading. Therefore, the deformations of the bridge were examined under four distinct load cases. In each case, the variable truck load was altered while all other loads were held constant. Figures 5.13 to 5.20 present the applied truck load configurations for each load case, accompanied directly below by the corresponding deformation response of the model. All Figures depict a side (XZ-plane) view of the bridge. To facilitate comparison, the deformation scale has been kept consistent across all Figures, using a scale factor of 500.

Figure 5.13 illustrates the bridge under self-weight only, with no truck load applied. As expected, the resulting deformation is minimal, as shown in Figure 5.14. Figures 5.15, 5.17, and 5.19 show three other load cases, each of which includes a variable load. In these cases, the largest deformations are clearly concentrated directly beneath the applied variable load, and the deformation is of similar magnitude. Overall, it can be concluded that the model exhibits a logical and realistic deformation response under all four load cases.

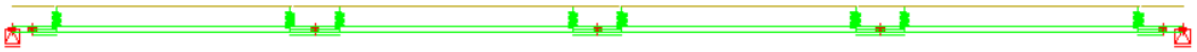

Figure 5.13: Variable loads for load case 1

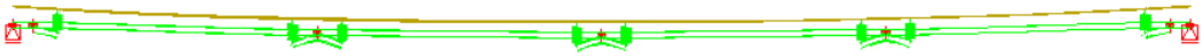

Figure 5.14: Deformation for load case 1 (x500)

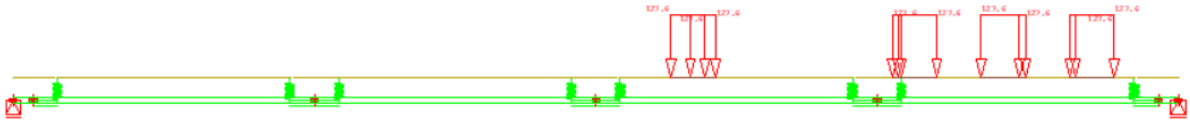

Figure 5.1536: Variable loads for load case 13

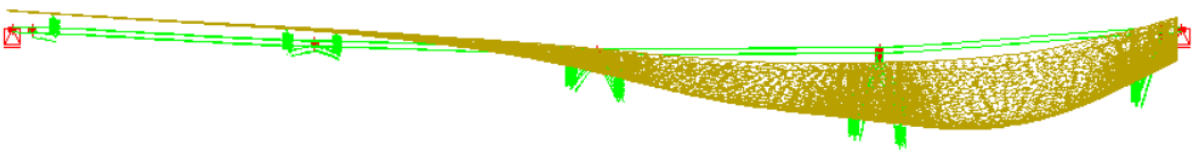

Figure 5.1637: Deformation for load case 13 (x500)

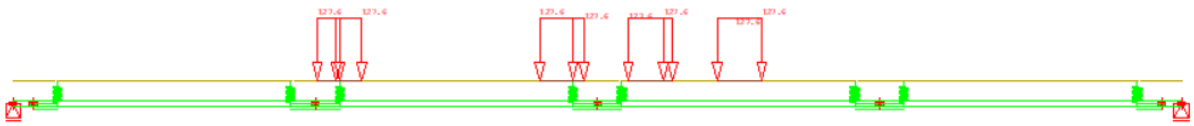

Figure 5.17: Variable loads for load case 21

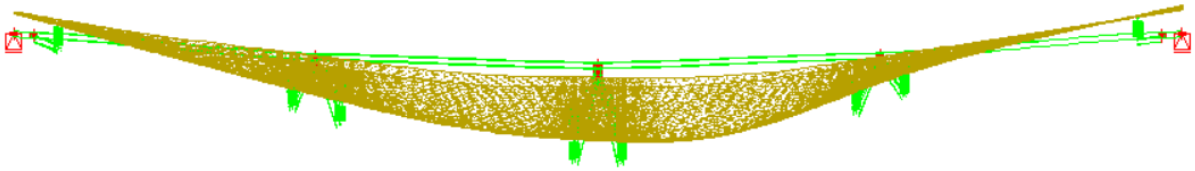

Figure 5.18: Deformation for load case 21 (x500)

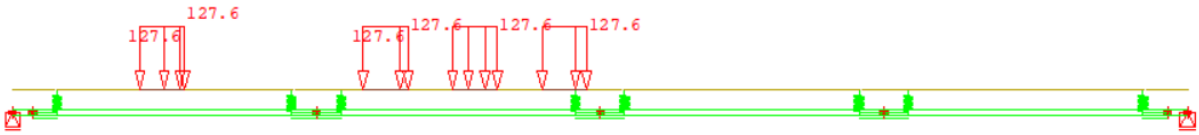

Figure 5.19: Variable loads for load case 25

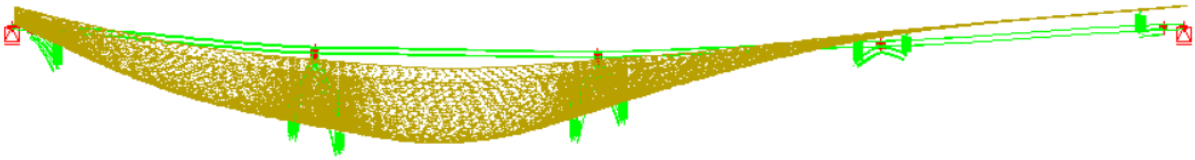

Figure 5.20: Deformation for load case 25 (x500)

5.5 Sensitivity

Because the measured force in bolt 2 differs from the force in the other bolts for various types of loading, the hypothesis mentioned in the previous chapter was tested to determine whether the forces in both types of bolts could be accurately predicted using the model. According to this hypothesis, the rubber interlayer between the bridge deck, crossbeam, and clamping plate was the cause of the differences in force between bolt 2 and the other bolts. By varying the stiffness of this interlayer in the model, its impact on the forces in the bolts was assessed.

Adjusting the stiffness of the rubber interlayer enabled an accurate prediction of the force cycles in all bolts using the model. It can therefore be concluded that the rubber interlayer influences the forces in the bolts. To better illustrate the relationship between the stiffness of the rubber interlayer and the magnitude of the force cycle in the bolts, the stiffness was further varied. This is shown in Figure 5.21, where it is evident that a higher stiffness of the connection results in a lower reaction force in the bolt.

A curve fit was applied to the relationship between the stiffness of the rubber interlayer and the bolt force to provide insight into the potential magnitude of the force in the bolt. This is shown in Figure 5.22. The derivative of this curve fit was taken to analyse the potential maximum force in the bolt. At a stiffness of -1750 mm per 1000 kN, the derivative is nearly horizontal (slope of 0.01). The deformation of the rubber for this low stiffness is approximately 1 mm, this is a realistic value for this rubber layer that has a thickness of 10 mm. At this stiffness, a force variation of 6.60 kN occurs during the force cycle, corresponding to a stress of 32.83 N/mm² in the bolt. This falls below the cut-off limit of 37.25 N/mm² mentioned in the previous chapter. This means that even at this very low connection stiffness, the force cycle in the bolt does not impact the bolt's service life. This force cycle is lower than the force cycle of 9-90 kN applied by J. Köhlenberg, which did not have an effect on the service life of the iSRR connector (J. Köhlenberg, 2023). So it can be concluded that for the lowest stiffness the connector's service life will not be affected.

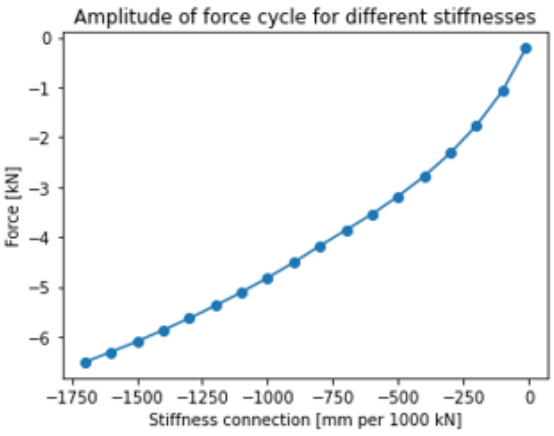

Figure 5.21: Amplitude of the force cycle

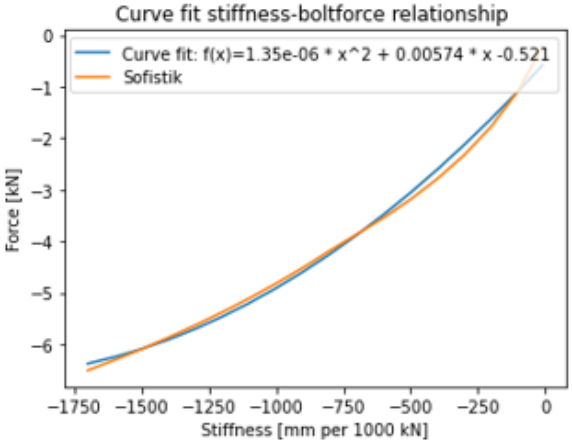

Figure 5.22: Sensitivity of the stiffness-bolt force relationship

6. Conclusions

In the preceding chapters, various conclusions were drawn, these are summarized below:

- Both types of connectors experience a significant loss of preload immediately after installation due to the presence of the rubber interlayer. After one day, only 77.5% of the initial preloading force remains. This considerable initial loss is caused by the rubber interlayer that is located between the clamping plate and the bridge deck.

- After 250 days, the iSRR connector retains, on average, 50.6% of its original preloading force. Which means that on average 17.7 kN of the original 35 kN of preload in still present after this period. The connector performs slightly better than the Lindapter bolt connector, which retains 42.7% of the original preloading force after the same period. This is 14.9 kN of the original 35 kN preload present.

- The amount of preload force in the bolt does not impact the magnitude of the response to either traffic loads or loads caused by the opening and closing of the bridge, for both connector types.

- The force variations in the bolts are relatively small compared to the applied loads. This is due to the design of the connectors, where a clamping plate has been applied so the connector only transfers tensile forces. The maximum stress variation in the bolts due to traffic loading is 9.70 N/mm^2. This value is below the cut-off limit, which is 37.25 N/mm^2, according to Eurocode 3, therefore have the load cycles due to traffic loading no impact on the lifespan of the bolts for both connector types.

- The difference in the response in the bolt due to varying truck speeds is less than 0.05 kN for both connector types. Therefore, traffic speed has a negligible effect on the magnitude of forces experienced by the bolts in both the iSRR and Lindapter bolt connector.

- Both connector types experience a similar response to variations in temperature. Higher temperatures lead to increased tensile force in the bolts, while lower temperatures result in reduced tensile forces. A change of temperature of 15 °C leads to force changes in the bolt of around 2.5 kN.

- There is a relationship between the stiffness of the rubber interlayers and the amplitude of the load cycle in the bolted connector due to traffic loading. Using the finite element model, there can be concluded that even for the most unfavourable stiffness conditions of the rubber interlayers, the load cycles, with a maximum of 32.83 N/mm^2, still remain under the cut-off limit of 37.25 N/mm^2 and therefore have no effect on the lifespan of the bolts.

- The forces in the bolts for both type of connectors can accurately be predicted with a finite element model. The model can be used to investigate the bolt forces when further extrapolating the applied load.

7. Recommendations

A couple of recommendations for future research are stated below:

- The rubber interlayer at the bolt between the clamping plate and the FRP bridge deck has significant influence on the loss of preload of both connectors. To investigate the loss of preload of the connectors itself, it would be interesting to monitor the loss of preload for both connectors with the rubber interlayer only present further from the bolt. This could help assessing whether the positioning of the rubber interlayer between the clamping plate and the bridge deck can be optimised.

- The force cycles, due to both traffic loading and opening of the bridge, in Lindapter bolt 2 are significantly different in magnitude than the force cycles in the other bolts. It could be interesting to examine whether the contact between the clamping plate and the crossbeam is sufficient for all of the connectors.

- Rubber is a complicated material that behaves nonlinear and has varying responses to loading. The time-dependent properties of rubber have not been taken into account in the finite element model. Investigating this more thoroughly could be valuable for improving the accuracy of the long-term predictions of the connector forces.

Bibliography

1993-1-9+C2, N.-E. (2012). *Eurocode 3: Design of steel structures -.*

A. Christoforidou, M. P. (2024). *Fatigue performance of composite-steel injected connectors at room and elevated temperatues.* TU Delft.

A. Manalo, T. A. (2016). *State-of-the-Art Review on FRP Sandwich Systems for Lightweight Civil Infrastructure.*

Avilés, F. (2008). *Experimental studies of compression failure of sandwich specimens with face/core debond.* Florida Atlantic University.

Csillag, F. (2018). *Demountable deck-to-girder connection of FRP-steel hybrid bridges.* TU Delft.

Eckold, G. (1994). Design and Manufacture of Composite Structures. Woodhead.

F. Csillag, M. P. (2021). *Push-out behaviour of demountable injected vs. blind-bolted connectors in FRP decks.* TU Delft.

G. Olivier, F. C. (2023). *Feasibility of bolted connectors in hybrid FRp-steel structures.* TU Delft.

H. Awais, Y. N. (2020). *Environmental benign natural fibre feinforced thermoplastic composites: A review.* Universiti Sain Malaysia.

J. Köhlenberg, M. P. (2023). *Design of demountable iSRR connectors on oversized holes subjected to wheel loading.* TU Delft.

K. Abdurohman, M. S. (2018). *Effect of mesh-peel ply variation on mechanical properties of E-glas composite by infusion vacuum method.*

K. Gunaydin, C. R. (2022). *Energy absorption enhancement of additively manufactured hexagonal and re-entrant (auxetic) lattice structures by using multi-material reinforcements.*

K. Park, S. K. (2006). *Degree of composite action verification of bolted GFRP bridge deck-to-girder connection system.*

Landrock, S. E. (2009). *Adhesives Technology Handbook.*

M. Fotouhi, S. S. (2015). *Analysis of the damage mechanisms in mixed-mode delamination of laminated composites using acoustic emission data clustering.*

Nijgh, M. (2017). *New Materials for Injected Bolted Connections.* TU Delft.

Olivier, G., Csillag, F., Tromp, E., & Pavlovic, M. (2021). *Conventional vs. reinforced resin injected connectors' behaviour in static,.* Delft: Elsevier.

Pipinato, A., Pellegrino, C., & Modena, C. (2012, September 12). Fatigue Behaviour of Steel Bridge Joints Strenghtened with FRP Laminates. *Modern Applied Science*.

Rijkswaterstaat. (2021, March 20). *Roadmap beweegbare bruggen*. Opgehaald van rwsinnoveert: https://rwsinnoveert.nl/focuspunten/vervanging-renovatie/beweegbare-bruggen/

Schultz van Haegen-Maas Geesteranus, M. (2016, 11 29). *Vaststelling van de begrotingsstaten van het Ministerie van Infrastructuur en Milieu (XII) voor het jaar 2017.* Opgehaald van officielebekentmakingen: https://zoek.officielebekendmakingen.nl/kst-34550-XII-60.html

Sofistik. (2023).

Thomas Keller, H. G. (2006). *In-plane compression and shear performance of FRP bridge decks acting as top chord of bridge girders.* Swiss Federal Institute of Technology.

Vinson, J. R. (2005). *Sandwich Structures: Past, Present, and Future.* University of Delaware.

X. Jiang, M. K. (2012). *Study on mechanical behaviors of FRP-to-steel adhesively-bonded joint under tensile loading.* TU Delft.

Zureick, A. (1995). *Fiber-reinforced Polymeric Bridge Decks.*

Annex A Dimensions of the girder and crossbeam

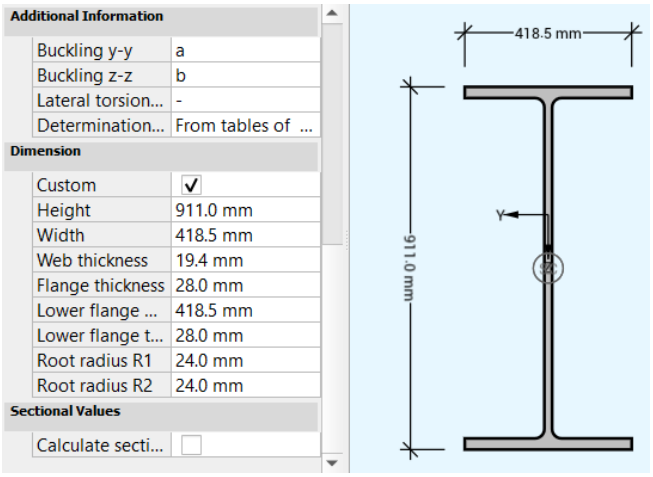

Dimensions of the longitudinal girder

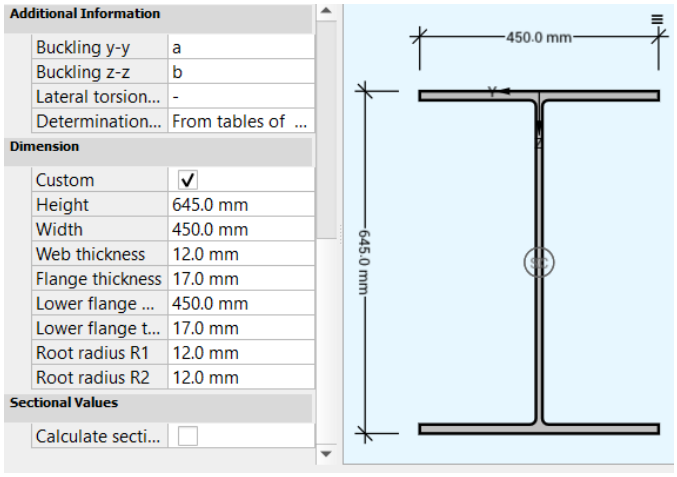

Dimensions of the middle of the crossbeam

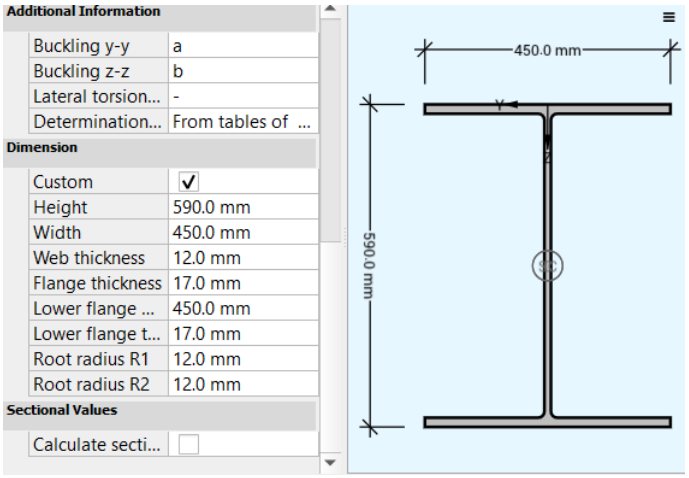

Dimenions of the ends of the crossbeam